

Stephen F. Austin State University

**SFA ScholarWorks**

---

Electronic Theses and Dissertations

---

12-2018

## DEPOSITIONAL ENVIRONMENT AND FACIES ANALYSES OF THE OWL MOUNTAIN PROVINCE, FORT HOOD MILITARY INSTALLATION, BELL AND CORYELL COUNTIES, TEXAS

Jacob Meinerts

meinertsja@jacks.sfasu.edu

Follow this and additional works at: <https://scholarworks.sfasu.edu/etds>



Part of the [Geology Commons](#), [Geomorphology Commons](#), [Hydrology Commons](#), and the [Sedimentology Commons](#)

Tell us how this article helped you.

---

### Repository Citation

Meinerts, Jacob, "DEPOSITIONAL ENVIRONMENT AND FACIES ANALYSES OF THE OWL MOUNTAIN PROVINCE, FORT HOOD MILITARY INSTALLATION, BELL AND CORYELL COUNTIES, TEXAS" (2018). *Electronic Theses and Dissertations*. 222.  
<https://scholarworks.sfasu.edu/etds/222>

This Thesis is brought to you for free and open access by SFA ScholarWorks. It has been accepted for inclusion in Electronic Theses and Dissertations by an authorized administrator of SFA ScholarWorks. For more information, please contact [cdsscholarworks@sfasu.edu](mailto:cdsscholarworks@sfasu.edu).

---

DEPOSITIONAL ENVIRONMENT AND FACIES ANALYSES OF THE OWL  
MOUNTAIN PROVINCE, FORT HOOD MILITARY INSTALLATION, BELL AND  
CORYELL COUNTIES, TEXAS

Creative Commons License



This work is licensed under a [Creative Commons Attribution-Noncommercial-No Derivative Works 4.0 License](https://creativecommons.org/licenses/by-nc-nd/4.0/).



**DEPOSITIONAL ENVIRONMENT AND FACIES ANALYSES OF THE OWL  
MOUNTAIN PROVINCE, FORT HOOD MILITARY INSTALLATION, BELL AND  
CORYELL COUNTIES, TEXAS**

By

Jacob Allan Meinerts, B.S

Presented to the Faculty of the Graduate School of

Stephen F. Austin State University

In Partial Fulfillment

Of the Requirements

For the Degree of

Masters of Science

STEPHEN F. AUSTIN STATE UNIVERSITY

December 2018

**Depositional Environment and Facies Analyses of the Owl Mountain  
Province, Fort Hood Military Installation, Bell and Coryell Counties, Texas**

By

JACOB ALLAN MEINERTS, B.S.

APPROVED:

---

Dr. Melinda S. Faulkner, Thesis Director

---

Dr. Kevin W. Stafford, Committee Member

---

Dr. LaRell Nielson, Committee Member

---

Dr. Joseph A. Musser, Committee Member

---

Pauline M. Sampson, Ph.D.  
Dean of Research and Graduate Studies

## **ABSTRACT**

The Owl Mountain Province is a plateaued, karst landscape located in the eastern section of the Fort Hood Military Installation and is characterized by Lower Cretaceous Fredericksburg Group carbonates. The topography is capped by thick sequences of the Edwards limestone; steep scarps and incised valleys along the edges of the plateaus host inter-fingering outcrops of the Edwards and Comanche Peak limestones, and the lower valleys are covered by alluvial sediments and intermittent outcrops of the Walnut Clay. These formations were deposited to the north and west of the main Edwards trend, and are thought to be part of a series of complex carbonate mounds that developed as backreef deposits in a restricted environment on the Comanche Shelf, associated with the western flank of the Belton High.

The purpose of this study is to describe the microfacies within the Fredericksburg Group and characterize the depositional environment of the study area. Field observations and laboratory analyses were used to investigate the microfacies in greater detail to provide evidence relating to the compositional makeup and diagenetic processes of the Lower Cretaceous strata. Sixteen lithostratigraphic sections were measured in the Comanche Peak and Edwards formations, identifying microfacies through field descriptions based on allochems, matrix, bioturbation, bedding style, and other distinct features. After thin section

analyses, 11 microfacies were identified, characterized, and used to create a diagenetic model to provide an accurate depiction of the Lower Cretaceous middle shelf depositional environment of the Owl Mountain Province.

## **ACKNOWLEDGEMENTS**

I would like to thank all of the people that have helped make this project a reality, mainly my advisor on this journey, Dr. Mindy Faulkner. If she hadn't convinced me to come to graduate school I don't know where I would be or what I would be doing, her guidance throughout this project has been unparalleled. I would also like to thank Dr. Kevin Stafford for all of his help on this project as well, I know I annoyed him with all of my diagenesis and thin section questions. Many of my friends and fellow graduate students helped in the field collecting samples and data, thank you to Colby Reece, Jessica Shields, Kaleb Henry, and Heather Dailey. I would also like to thank Charles Pekins, who was our liaison on the base, none of this work is possible without his cooperation and his desire for scientific research within the base. The Department of Geology also deserves a big thank you, my work isn't possible without the department's help and funding. Lastly I would like to thank my family and friends for their support of me furthering my education these last few years.

## TABLE OF CONTENTS

	Page
ABSTRACT.....	i
ACKNOWLEDGEMENTS.....	iii
TABLE OF CONTENTS.....	iv
LIST OF FIGURES.....	ix
LIST OF TABLES.....	xiii
PREFACE.....	xv
DEPOSITIONAL ENVIRONMENT AND FACIES ANALYSES OF THE OWL MOUNTAIN PROVINCE, FORT HOOD MILITARY INSTALLATION, BELL AND CORYELL COUNTIES, TEXAS.....	1
ABSTRACT.....	1
INTRODUCTION.....	2
GEOLOGIC SETTING.....	5
STUDY AREA.....	7

	Page
REGIONAL DEPOSITIONAL ENVIRONMENT.....	10
METHODOLOGY.....	13
MICROFACIES ANALYSES.....	17
PERITIDAL MUD FLAT MICROFACIES.....	17
PERITIDAL – BIOHERMAL MICRO FACIES.....	20
SUBTIDAL TO LAGOONAL – MOBILE GRAIN FLAT AND BACKREEF LAGOON MICROFACIES.....	23
OWL MOUNTAIN PROVINCE DEPOSITIONAL MODEL...	25
DIAGENETIC MODEL.....	32
CONCLUSIONS.....	36
REFERENCES.....	39
APPENDIX (A) EXTENDED PREVIOUS WORKS.....	42
PREVIOUS MODELS	42
APPENDIX (B) MEASURED SECTIONS .....	48

	Page
MAP OF MEASURED SECTION LOCATIONS.....	49
SECTION 1.....	50
SECTION 2.....	51
SECTION 3.....	52
SECTION 4.....	53
SECTION 5.....	54
SECTION 7.....	55
SECTION 8.....	56
SECTION 9.....	57
SECTION 10.....	58
SECTION 11.....	59
SECTION 12.....	60
SECTION 13.....	61

	Page
SECTION 14.....	62
SECTION 15.....	63
SECTION 16.....	64
APPENDIX (C) THIN SECTION ANALYSES.....	65
MAP OF THIN SECTION LOCATIONS.....	66
JM01.....	67
JM02.....	68
JM03.....	69
JM04.....	70
JM05.....	71
JM06.....	72
JM07.....	73
JM08.....	74

	Page
JM09.....	75
JM10.....	76
JM11.....	77
JM12.....	78
JM13.....	79
JM14.....	80
JM15.....	81
VITA.....	82

## LIST OF FIGURES

	Page
Figure 1: Paleogeographic map of Texas during the Cretaceous. Light blue = shallow water, dark blue = deeper water, green = Kirschberg Lagoon.....	4
Figure 2: Map showing Fort Hood Military Installation in green with Owl Mountain Province in light blue, city of Killeen, major highways, and counties labeled, source: ArcGIS online database.....	9
Figure 3: Regional depositional model for the greater Killeen area during the Cretaceous, study area outlined in red (modified from Kerr 1977 and Brown 1975). .....	12
Figure 4: Map showing the location of each measured section within the study area, source: ArcGIS online database.....	15
Figure 5: Measure section 8 drafted in Adobe Illustrator, showing the vertical transitions between subtidal/lagoonal to peritidal facies.....	16
Figure 6: Microphotographs of the mudflat microfacies.....	19
Figure 7: Outcrop photo showing nodular chalky beds (zone A) and massive crystalline beds (zone B).....	20
Figure 8: Microphotographs of the bioherm microfacies.....	22

	Page
Figure 9: Microphotographs of the mobile grain flat microfacies.....	25
Figure 10: Depositional model for the Owl Mountain Province.....	28
Figure 11: Map showing the measured sections that were used to construct the A – A' cross section (figure 12).....	30
Figure 12: Theoretical cross section showing the facies groups in the study area. ....	31
Figure 13: Diagenesis model showing timeline from deposition to present time with diagenetic features listed.....	33
Figure A-1: Depositional model of the Edwards Limestone in the area of Belton, Texas, (from Kerr, 1977).....	43
Figure A-2: Conceptual model of mound structure with facies development, (from Bryant 2012; modified from Amsbury et al. 1984).....	46
Figure A-3: Seepage-reflux model for dolomitization (from Fisher and Rodda, 1969).....	47
Figure B-1: Map of measured section locations.....	49
Figure B-2: Microfacies column of measured section 1.....	50
Figure B-3: Microfacies column of measured section 2.....	51

	Page
Figure B-4: Microfacies column of measured section 3.....	52
Figure B-5: Microfacies column of measured section 4.....	53
Figure B-6: Microfacies column of measured section 5.....	54
Figure B-7: Microfacies column of measured section 7.....	55
Figure B-8: Microfacies column of measured section 8.....	56
Figure B-9: Microfacies column of measured section 9.....	57
Figure B-10: Microfacies column of measured section 10.....	58
Figure B-11: Microfacies column of measured section 11.....	59
Figure B-12: Microfacies column of measured section 12.....	60
Figure B-13: Microfacies column of measured section 13.....	61
Figure B-14: Microfacies column of measured section 14.....	62
Figure B-15: Microfacies column of measured section 15.....	63
Figure B-16: Microfacies column of measured section 16.....	64

	Page
Figure C-1: Map showing thin section locations.....	66

## LIST OF TABLES

	Page
Table 1: List of microfacies depicted in depositional model for the Owl Mountain Province.....	29
Table C-1: Thin section photos and classification of thin section JM01	67
Table C-2: Thin section photos and classification of thin section JM02	68
Table C-3: Thin section photos and classification of thin section JM03	69
Table C-4: Thin section photos and classification of thin section JM04	70
Table C-5: Thin section photos and classification of thin section JM05	71
Table C-6: Thin section photos and classification of thin section JM06	72
Table C-7: Thin section photos and classification of thin section JM07	73
Table C-8: Thin section photos and classification of thin section JM08	74
Table C-9: Thin section photos and classification of thin section JM09	75
Table C-10: Thin section photos and classification of thin section JM10	76

	Page
Table C-11: Thin section photos and classification of thin section JM11	77
Table C-12: Thin section photos and classification of thin section JM12	78
Table C-13: Thin section photos and classification of thin section JM13	79
Table C-14: Thin section photos and classification of thin section JM14	80
Table C-15: Thin section photos and classification of thin section JM15	81

## **PREFACE**

The research done in this study was conducted within Fort Hood Military Installation which lies within the Lampasas Cut Plain and hosts an abundance of Edwards carbonate strata. This work was done in conjunction with the Fort Hood Natural Resources Management Branch of the United States Army in order to further the understanding of the geology within Fort Hood Military Installation, as well as to further understand complex carbonate strata and how the surrounding environments affect them.

This thesis has been prepared in accordance with publishing guidelines established by the Carbonate and Evaporites Journal and will be submitted by December 15, 2018 for publishing consideration. In addition to this research, an overview of regional studies pertaining to the Fredericksburg Group depositional environment can be found in Appendix A. Appendices B and C contain detailed microfacies and petrographic analyses considered in this research.

**DEPOSITIONAL ENVIRONMENT AND FACIES ANALYSES OF THE OWL  
MOUNTAIN PROVINCE, FORT HOOD MILITARY INSTALLATION,  
BELL AND CORYELL COUNTIES, TEXAS**

**Abstract**

The Owl Mountain Province is a plateaued, karst landscape located in the eastern section of the Fort Hood Military Installation and is characterized by Lower Cretaceous Fredericksburg Group carbonates. The topography is capped by thick sequences of the Edwards limestone; steep scarps and incised valleys along the edges of the plateaus host inter-fingering outcrops of the Edwards and Comanche Peak limestones, and the lower valleys are covered by alluvial sediments and intermittent outcrops of the Walnut Clay. These formations were deposited to the north and west of the main Edwards trend, and are thought to be part of a series of complex carbonate mounds that developed as backreef deposits in a restricted environment on the Comanche Shelf, associated with the western flank of the Belton High.

The purpose of this study is to describe the microfacies within the Fredericksburg Group and characterize the depositional environment of the study area. Field observations and laboratory analyses were used to investigate the microfacies in greater detail to provide evidence relating to the compositional

makeup and diagenetic processes of the Lower Cretaceous strata. Sixteen lithostratigraphic sections were measured in the Comanche Peak and Edwards formations, identifying microfacies through field descriptions based on allochems, matrix, bioturbation, bedding style, and other distinct features. After thin section analyses, 11 microfacies were identified, characterized, and used to create a diagenetic model to provide an accurate depiction of the Lower Cretaceous middle shelf depositional environment of the Owl Mountain Province.

## **Introduction**

The Owl Mountain Province hosts Fredericksburg Group carbonate strata deposited in the Lower Cretaceous during successive transgressive/regressive cycles; within the study area, the Edwards and Comanche Peak formations are the primary lithostratigraphic units. The Edwards limestone is widespread across Texas, and presents as varied microfacies depending on the environment in which it was deposited including massive, fossiliferous beds as well as nodular, chalky beds and dolostone (Rose, 1972). The Comanche Peak formation is a nodular, chalky limestone which underlies the Edwards, and the two formations exhibit an inter-fingering relationship in the study area (Rose, 1972).

The Edwards strata in the study area was deposited in a unique environment on the Comanche Shelf. The area was protected by the Central Texas Reef Trend to the northwest as well as the Stuart City Trend to the south.

The study area is thought to be an outlier of the main reef trend, forming along the margin or flank where shoals and smaller patch reefs and bioherms or mounds formed (Figure 1; Amsbury et al., 1984; Brown, 1975). To the northeast, the North Texas Tyler Basin contained deeper water and current activity from this basin would move inland to form channels between reefs. To the southwest, the Kirschberg Lagoon formed which may have influenced the study area as sea level dropped and supratidal microfacies prograded into the area. Microfacies analyses and diagenetic modeling of Lower Cretaceous strata helped characterize the middle shelf environment that existed in the Owl Mountain Province.



## **Geologic Setting**

The southeastern margin of the Comanche Shelf was flanked by the Stuart City Reef complex, which formed as a barrier reef along the shoreline of the ancestral Gulf of Mexico (Roberson, 1972). To the northwest of the Stuart City Trend, the Edwards limestone, regionally considered a backreef facies (Roberson, 1972), was deposited on the Comanche Shelf; in the northeastern extent of the Comanche Shelf, patch reefs and bioherms extend across the area as the Central Texas Reef Trend (Figure 1). The shelf provided a stable, protected environment for smaller, more numerous elongate and lobate patch reefs and bioherms (Damman, 2011; Roberson, 1972). This area of biohermal mounds and patch reefs was bounded on the north, northeast, and south by basins of deeper water, and to the west by the Llano Uplift and Kirschberg Lagoon (Fisher and Rodda, 1969).

Previous works postulate that the environment of deposition was calm to slightly agitated from tidal flats and channels coming in from the northeast, evidenced by the abundance of micrite and fine carbonate mudstone (Roberson, 1972; Plumley et al. 1962). The mostly intact nature of the fossils and the presence of fecal pellets within the reef rock also suggests a calm environment. Swale and ripple marks suggest wave action over the reef area, and ammonite casts among the reef rock also suggest currents or waves strong enough to transport large shells (Roberson, 1972). The combination of the low energy to slightly agitated environments were ideal conditions for the deposition of the

Edwards limestone within the study area. The water temperature was warm with consistent temperatures calculated to be 32-34°C, possibly higher, (Damman, 2010; Forster, 2007; Steuber et al., 2005; Wilson and Norris, 2001). The lack of corals present during this time also suggests that the temperatures were warmer than 30°C, though they are more abundant to the southeast in deeper waters (Damman, 2010; Scott, 1990a). The rudist reefs of Central Texas exhibit low biodiversity, with only 18 species of rudist identified, compared to the 792 total species identified in the Middle East and Mediterranean (Damman, 2010; Steuber, 1999). Other than rudists, only a few species of echinoderms, bivalves, gastropods, bryozoans, foraminifera, and algae have been identified (Damman, 2010). The salinity of the waters was fairly high, even hypersaline at times, with an average salinity of 36.2-36.6 parts per thousand (Forster, 2007). The saline conditions and warm water contributed to the low biodiversity of the reefs, as rudists were able to withstand harsher conditions than the corals. The deposition of the reef structures in the Edwards was controlled by sea level as reef growth was directly dependent on water levels (Damman, 2010; Roberson, 1972). The bioherms in the area varied; most were between 10-100m in diameter, with a height not to exceed the estimated water depths of 7-8m (Damman, 2010; Bedout and Loucks, 1974; Young, 1959). Jacka and Brand (1977) proposed that the Edwards limestone was subaerially exposed up to 40m; oxidation, case hardening, borings, and the presence of paleosols at the top of the Edwards within the area are evidence of dropping sea level and potential exposure. The

Kiamichi Shale formation onlaps the Edwards Formation unconformably, though the Kiamichi may not be present over some of the patch reefs due to variable relief provided by the Belton High (Nelson, 1959).

Damman (2011), compared the patch reefs of Central Texas to the modern Bermuda coral reefs. Many factors of each reef system were similar, including climate, salinity, energy, turbidity, current, reef geometry, bioherm size, reef depth, reef protection, biodiversity, zonation factors, and grain size (Damman, 2011). The only key difference between the two reef environments was water temperature. The Bermuda reefs are considered to be “cold water” reefs with winter temperatures on the outer reefs falling to as low as 18°C; though for much of the year they are a much warmer 25° to 28°C (Forbes, 2011; Damman, 2010).

### **Study Area**

The Owl Mountain Province covers approximately 90 km<sup>2</sup>, and is located in the eastern section of the Fort Hood Military Installation in Bell and Coryell counties within the Lampasas Cut Plain (Figure 2). The province is a karst landscape characterized by Cretaceous-age limestone plateaus and canyons with rock outcrops, cliffs, sinkholes, caves, springs, and rock shelters. The plateaus are capped by thick sequences of Lower Cretaceous limestone and dolostone known traditionally and informally as the “Edwards,” which would have

been deposited to the south of the Central Texas Reef Trend. Outliers such as the Owl Mountain Province were separated from the main reef trend, and have been described as isolated mounds or shoals that developed on the Comanche Shelf near the Belton High in restricted circulation between the North Texas-Tyler Basin and the evaporitic material deposited in the Kirschberg Lagoon (Rose 1972). The strata in the study area is postulated to have been deposited within this unique and protected environment.

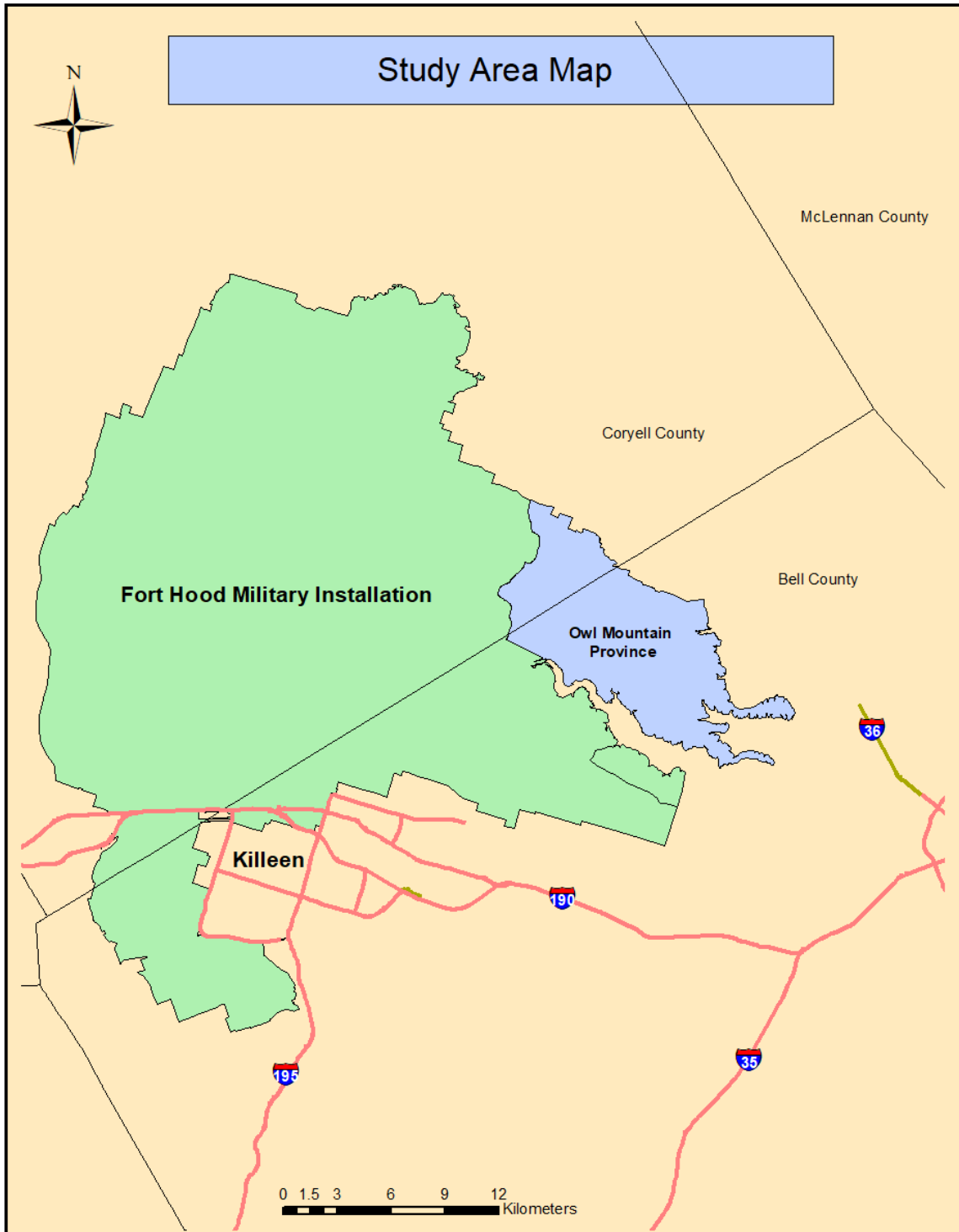


Figure 2: Map showing Fort Hood Military Installation in green with Owl Mountain Province in light blue, city of Killeen, major highways, and counties labeled, source: ArcGIS online database.

## **Regional Depositional Environment**

A regional model was developed to show the depositional environments that existed in the Central Texas area during the Lower Cretaceous. This model was developed using field and laboratory data associated with this study, coupled with models developed from previous works (Figure 3; Amsbury et al., 1984; Kerr, 1977; Brown, 1975) to characterize the region as accurately as possible. The model developed by Kerr (1977) covers the city of Belton regionally, showing the progradation of the inner and middle shelf environments outwards towards the basin as sea level drops. Brown (1975) studied the Moffatt Mound area, located east of the study area across Lake Belton. He found that there were up to eight different depositional environments in his area, ranging from supratidal to open shelf. Amsbury et al. (1984) also studied the Moffatt Mound trend, finding that the trend was a massive oolitic and skeletal grainstone trending WNW-ESE for at least 80 km, and postulated that this body separated the marine environment from the tidal flat environment. Fisher and Rodda (1969) studied the dolomitization of the Edwards limestone in Central Texas, developing a seepage-reflux model. This model showed saline brines from the evaporite Kirschberg Lagoon had an influence on the Edwards, dolomitizing portions of the strata (Fisher and Rodda, 1969).

The middle shelf section of the model completed for this study was derived using data from the study area while the inner shelf section of the model primarily follows the model by proposed by Kerr (1977). This model shows inner

and middle shelf environments, including lagoonal, beach and shoreface, mudflats (moving from clean to fossiliferous), mobile grain flats, patch reefs, and the deeper water basin. The patch reefs take on two forms, elongate and semi-circular; the elongate reefs formed more basinward and their crescent moon shape is due to the influence of incoming currents from deeper basins. The lobate reefs formed behind the protection of the elongate reefs, allowing them to form rounded morphologies as the microfacies grew outwards. The mobile grain flat microfacies group was deposited just shoreward of the patch reefs and amongst them and is primarily composed of ooids, peloids, and bioclasts. These microfacies could have also been imbricated by the currents migrating in and out through channels between the patch reefs. Shoreward from the mobile grain flat microfacies is the peritidal mud flat microfacies group. This area is primarily composed of mudstone and wackestones and may contain more intact fossils and dolomitic units.

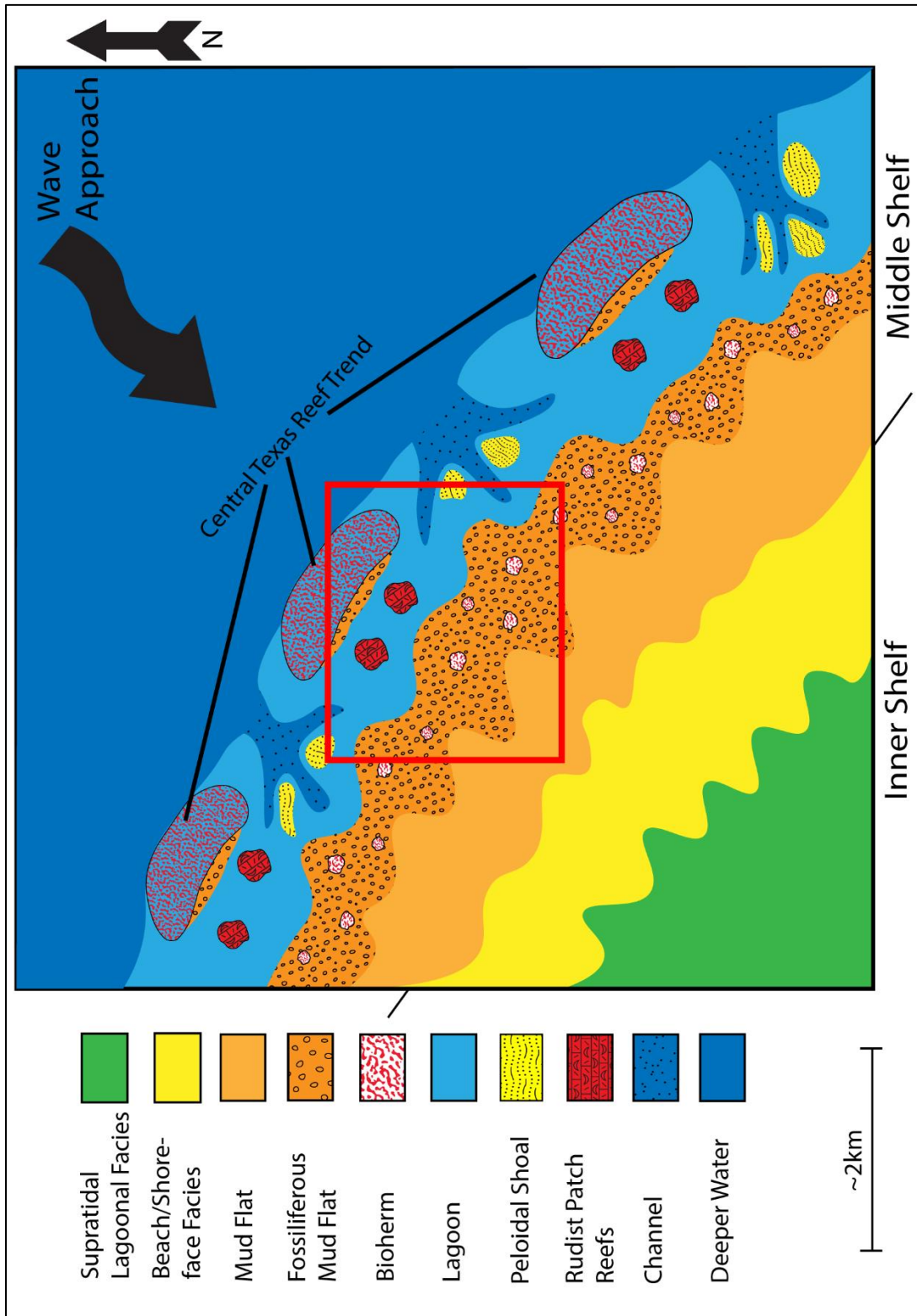


Figure 3: Regional depositional model for the greater Killeen area during the Cretaceous, study area outlined in red (adapted from Kerr 1977 and Brown 1975).

## **Methodology**

In order to characterize the microfacies in the study area and accurately describe the depositional environment, traditional field methods were coupled with petrographic research in the laboratory. In the field, outcrop analyses consisted of measured sections along road cuts, incised valleys, and cliffs that were safely accessible (Figure 4). Much of the land surface is covered with dense vegetation or soil and the amount of available rock section to observe is limited to natural scarps and those along manufactured outcrops created by road building and military training activities. Field assessment was conducted using a metric tape, rock hammer, and a hand lens; microfacies sections were described in the field detailing traditional features when measuring a stratigraphic section including: rock type (general and Dunham classification), fresh color, weathered color, grain size, allochems, sedimentary structures, bioturbation, bedding type, oxidation, mineralogy, and profile. A lithostratigraphic profile was constructed for each measured section to note any interesting and unusual features (Figure 5). Hand samples for each microfacies were collected and labeled for laboratory analyses.

After field measurements were complete, the hand samples were cut into 5cm x 2.5cm billets for laboratory analyses. Each billet was described in detail using an optical light microscope to determine microfacies characteristics. After a thorough analysis of each sample, the field and laboratory data were entered into a database and microfacies descriptions were grouped based on Dunham

classification, fresh and weathered colors, allochems, weathering profile, bedding type, and unique minerals and features. Each microfacies group was carefully analyzed to make sure the rock samples were similar in composition, and represented similar depositional environments. Once the final microfacies groups were confirmed, a sample representing each group was selected for thin section preparation by Spectrum Petrographics. Thin sections were described by using an optical light microscope to determine point counts and Folk classifications for each microfacies. Descriptions were compiled for each microfacies to help characterize the depositional environment and diagenetic features present in the samples.

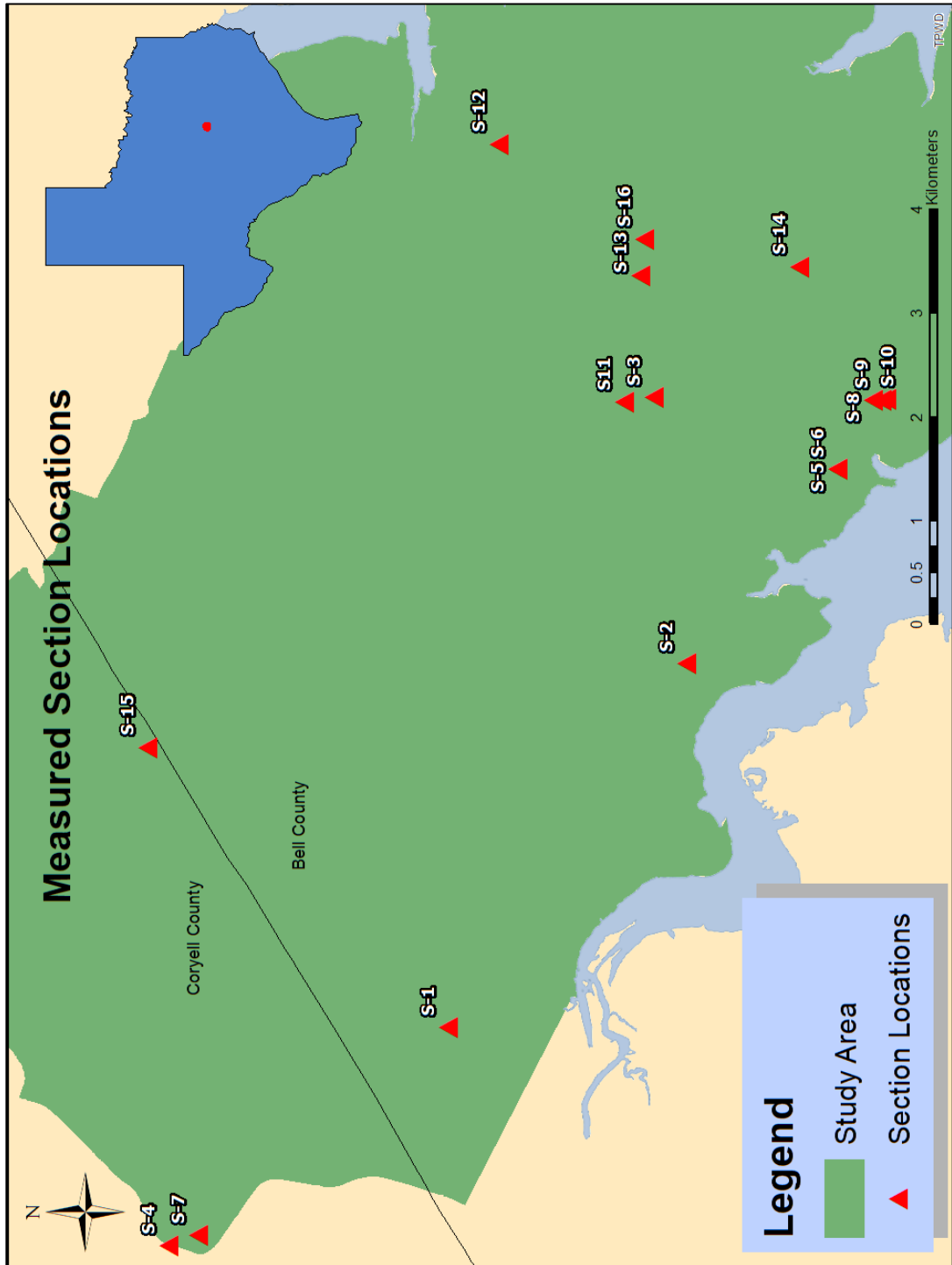


Figure 4: Map showing the location of each measured section within the study area, source: ArcGIS online database

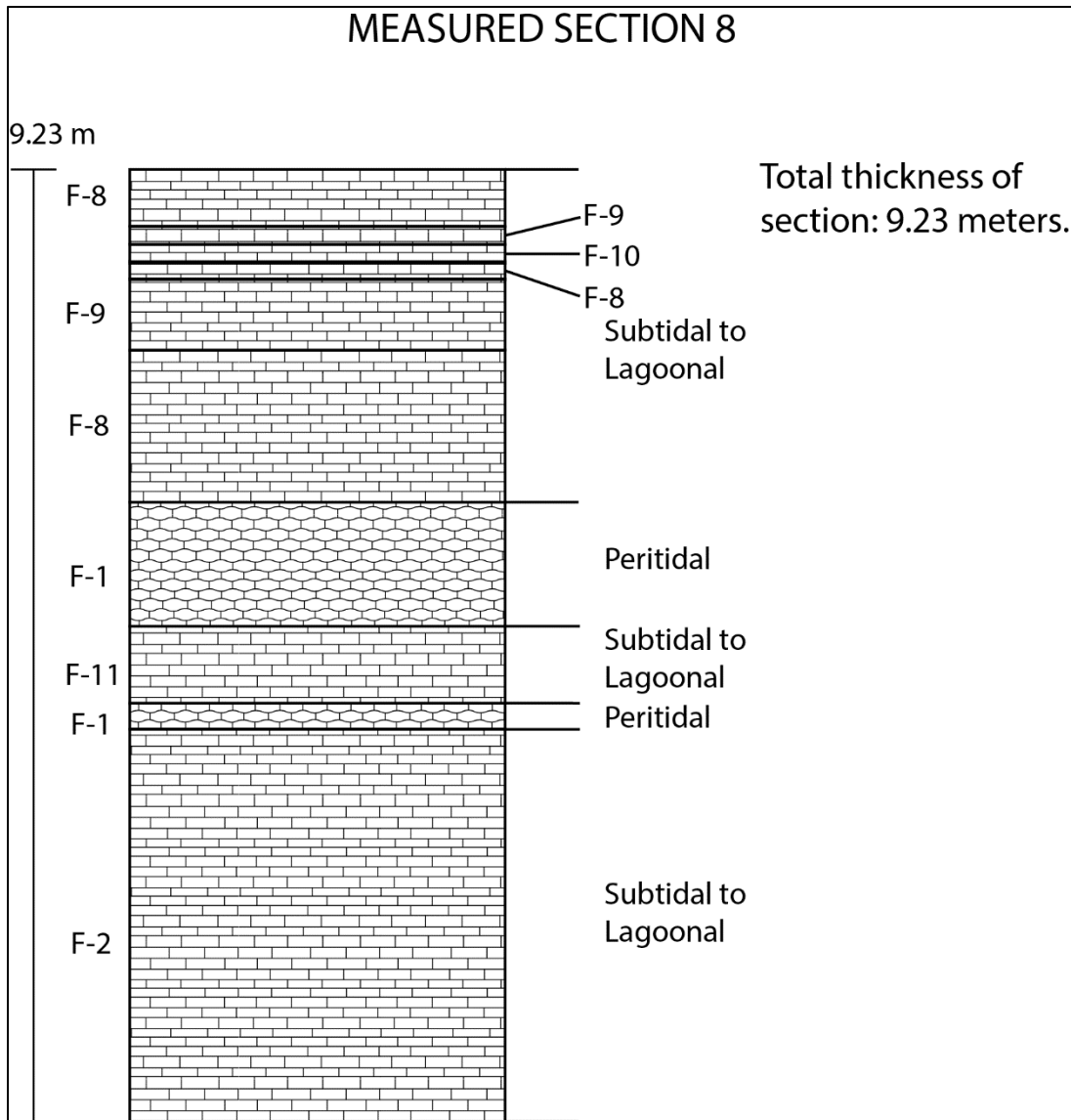


Figure 5: Measured section 8 drafted in Adobe Illustrator, showing the vertical transitions between subtidal/lagoonal to peritidal microfacies. F1- Sparse bioclastic mud flat microfacies, F2- dolomite mud flat microfacies, F3- peloidal shoal microfacies, F4- bivalve mud flat microfacies, F5- sheltered, back biohermal margin microfacies, F6- bivalve bioherm microfacies, F7- gastropod mud flat microfacies, F8- bioherm flank microfacies, F9- inter-biohermal channel microfacies, F10- sheltered, backreef/bioherm peloidal microfacies, F11- channel peloid microfacies.

## **Microfacies Analyses**

After laboratory analyses, 11 distinct microfacies were categorized into three depositional areas: peritidal mud flat, subtidal to lagoonal patch reefs, and subtidal to lagoonal mobile grain flat. Other features such as allochem content, abundance, and integrity were used to further differentiate the environments. The samples exhibited some variation in each depositional setting, which can be explained by their proximity to other features, such as a channel, patch reef, or the transition to another environment. The microfacies were categorized on the depositional model to demonstrate where they would have been within the overall setting of the middle shelf. In order to better understand the environment through time, diagenetic histories were interpreted for each thin section, and an overall diagenetic model was created for the area.

### **Peritidal Mud Flat Microfacies**

These microfacies were deposited in the shallow peritidal mud flat area and are commonly nodular and chalky in outcrop (Figure 7, Zone A) with large whole fossils found in some beds, and smaller broken fossils in others. The peritidal mudflat microfacies are commonly found interbedded between the stacking of massive and nodular beds commonly seen in the Comanche Peak and Edwards interfingering outcrops.

Microfacies 1 (F-1, Figure 6A) is a bioclastic mud flat facies, classified as a sparse biomicrite containing bivalves (4%), peloids (3%), and gastropods (2%). The allochems are small in size, with the majority being < 1mm, and are primarily broken within a micrite matrix and exhibit little porosity (< 1%). This microfacies is within the peritidal mud flat area that is nearing the transitional boundary to the subtidal-lagoonal area. The degree to which the allochems are broken as well as the smaller size of the allochems are evidence of this depositional environment. It is also possible that this area would be subject to wash up deposits from the subtidal-lagoonal area during storm events.

Microfacies 2 (F-2, Figure 6B) is a dolomite mud flat facies, classified as an unsorted biosparite and contains bivalves and peloids (1% each), and few bryozoan (<1%). The allochems varied in size from < 1mm to > 2mm. The matrix is dolomite cement (71%) with a smaller amount of calcite cement (7%) or micrite (22%), though the dolomite is a product of diagenesis. This microfacies is thought to have been deposited within the calmer mud flat area of deposition, as evidenced by low fossil content, and partial to whole allochems. The dolomite may indicate that this microfacies was deposited farther inland, as seepage reflux from the Kirschberg lagoon may have influenced dolomitization.

Microfacies 4 (F-4, Figure 6C) is a bivalve mud flat facies, classified as an unsorted biomicrite that contains bivalves (4%), gastropods (3%), and minor amounts of echinoids (1%). The allochems in this microfacies exhibit a slight increase in the number of bivalves and an increase in average size of the

fragments (> 1mm to < 2mm); the allochems in this microfacies are also less broken than in F-1. The F-4 microfacies would be in the peritidal mud flat depositional environment, most likely not far from F-1, but potentially more shoreward in slightly calmer waters.

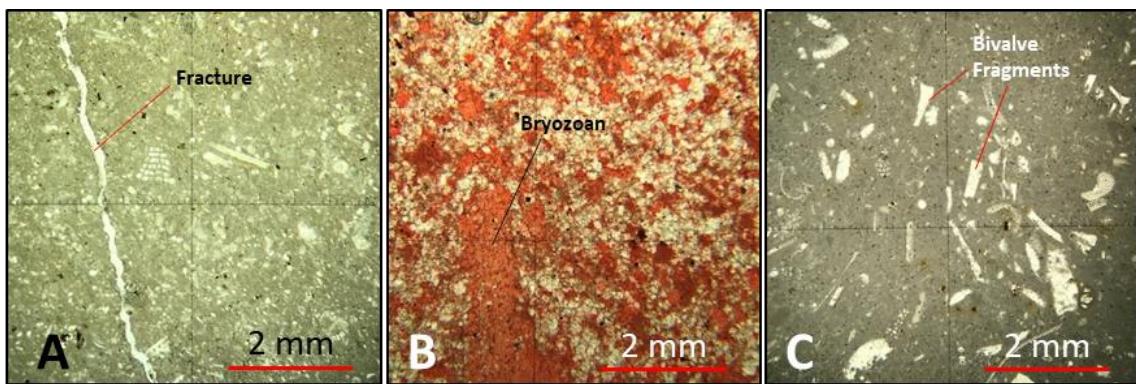


Figure 6: Mudflat microfacies, all microphotographs are in plane polarized light and viewed at 4x magnification. A) F-1 shows bivalve fragments, bryozoan, and rip up mud clasts within a micrite matrix, a fracture is seen going through the thin section as well. B) F-2 shows a dolostone with a bryozoan fragment. C) F- 4 has broken up fragments of bivalves within a micrite matrix.

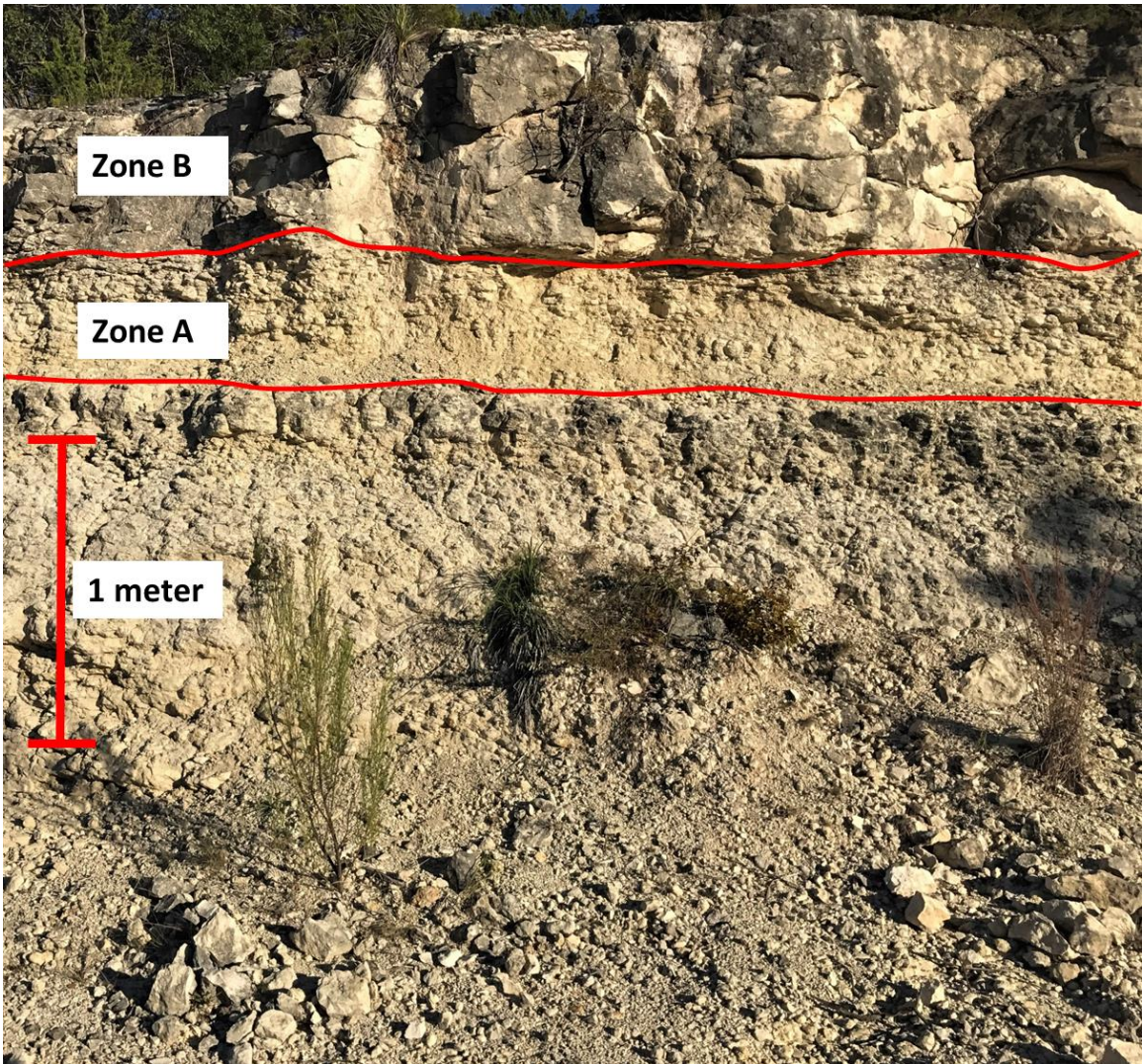


Figure 7: Outcrop photo showing nodular cherty beds (zone A) and massive crystalline beds (zone B).

### **Peritidal – Biohermal Microfacies**

These microfacies are widespread among the depositional setting depicted in the model created for this study (Figure 3). The microfacies in this group are representative of six of the thin sections analyzed for this research, and this microfacies could be applied to any of the bioherms, biohermal flanks, or

inter-bioherm channels, with the amount of major allochems slightly varying due to the degree of replacement or the presence of imbrication. These microfacies in outcrop are massive beds and form cliffs above the nodular peritidal microfacies units (Figure 7 Zone B)

Microfacies 6 (F-6, Figure 8A) is a bivalve biohermal facies classified as an unsorted biosparite and is directly associated with a bioherm environment based on the fossil content. It contains significant amounts of bivalves (17%) and peloids (12%), and lesser amounts of echinoderms (2%), foraminifera, algae, and bryozoan (all <1%). The allochems are closely packed, and are within a matrix composed of micrite (49%) and calcite cement (5%). This section contains moldic and vuggy porosity (12%), and minimal amount of dolomite cement (2%).

Microfacies 8 (F-8, Figure 8B) is a bioherm flank facies which contains bivalves (4-8%) and peloids (1-2%), as well as foraminifera (<1%). This microfacies contains a lesser amount of bivalves, though this is in part due to calcite replacement of most allochems. This microfacies contains large bivalve clasts, most replaced within a calcite spar cement matrix (57-84%) and exhibits a range of porosity (3-22%). Silicification is present as some allochems are replaced by opal, and some porosity has been infilled with quartz. This facies would have been deposited in association with a bioherm flank.

Microfacies 9 (F-9, Figure 8C) is an inter-bioherm channel facies. This microfacies also contains primarily bivalves (6%) and peloids (4%), and shows

sorting or imbrication, meaning it was deposited within a channel that flowed between patch reefs. This microfacies has 2-8% porosity, and has calcite (44-60%), dolomite (6-10%), and opal (3-35%) cements. This microfacies is thought to have been deposited in an inter-reef channel because it contains a significant amount of bivalves and doesn't contain a high number of peloids or ooids, which are associated with channels in the mobile grain flat zone.

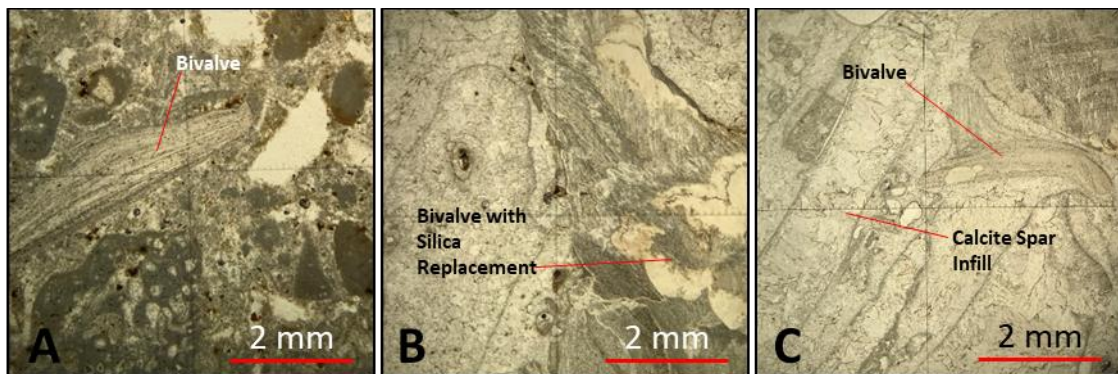


Figure 8: Subtidal/Lagoonal facies, all microphotographs are in plane polarized light and 4x magnification. A) F-6, shows a bioherm facies containing bivalves, algae, peloids, and moldic porosity. B) F-8, shows a large bivalve fragment that is semi replaced by silica. C) F-9, another bioherm facies, contains bivalves, and bioclasts replaced by calcite spar

### **Subtidal to Lagoonal - Mobile Grain Flat and Backreef Lagoon Microfacies**

The mobile grain flat depositional environment is identified by the high number of peloids or ooids, and can be unsorted or sorted, depending on the proximity to the mud flat zone. These microfacies covered a vast area of deposition throughout the subtidal to lagoonal zone, flowing in between the patch reefs with the channel flow as well as covering larger areas where breaks in the patch reef trend allowed stronger currents to flow, even reaching into and mixing

with the margin of the mud flat environment. These microfacies in outcrop are massive beds and form cliffs above the nodular peritidal microfacies beds (Figure 7, Zone B)

Microfacies 3 (F-3, Figure 9A) is a peloidal shoal facies, classified as an unsorted pelsparite primarily composed of peloids (75%) with some bivalves (1%). It contains little micrite (7%) or cement (3%) and has 12% porosity, both moldic and vuggy. This microfacies was deposited within the mobile grain flat depositional environment, as the sediments were migrating through the channels amongst the patch reefs. The scarce number of bivalves suggest that this microfacies was not in close proximity to the bioherms which were dominated by rudist bivalves.

Microfacies 10 (F-10, Figure 9B) is an unsorted peloidal facies associated with the mobile grain flat depositional environment, and is classified as an unsorted pelsparite. The primary constituent of this microfacies is peloids (35%), with small amounts of bivalves, gastropods, and bryozoan (1% each). The matrix is composed of primarily calcite cement (46%), dolomite (8%), and contains 5% porosity, primarily moldic with some vuggy porosity. The density of closely packed peloids suggests that this microfacies was deposited within the mobile grain flat environment, sheltered by patch reefs. The tight packing of allochems also suggests that this was deposited farther away from the mud flat area, centrally located within the mobile grain flat.

Microfacies 11 (F-11, Figure 9C) is a channel peloidal facies classified as a sorted pelsparite and contains primarily peloids (19%) and ooids (13%), with lesser amounts of bivalves (4%) and algae (1%). This microfacies also shows moldic and vuggy porosity (9%), and imbrication. The allochems in this microfacies are not densely packed and are within equant calcite spar cement (47%). This is the only major occurrence of ooids, in the majority of thin sections ooids have been dissolved away and only “ghost ooids” can be observed. The fact that this microfacies is less densely packed provides evidence for the depositional environment occurring close to the margin of the mud flat deposition zone. The sorting of the allochems provides evidence that the microfacies could have been at the termination of a channel as it met the mud flat zone.

Microfacies 7 (F-7, Figure 9D) is a gastropod mud flat facies classified as an unsorted biomicrite. It primarily contains gastropods (17%) and bivalves (16%) with minor amounts of algae and bryozoa (<1% each). This microfacies contains large, whole allochems (> 2mm) that are within a micrite matrix. This microfacies was deposited in calm water within a backreef lagoon where it was protected.

Microfacies 5 (F-5, Figure 9E) is a sheltered bioclastic lagoonal facies classified as an unsorted pelsparite, dominated by equant calcite cement with only 4% peloids and < 1% fossils. This section contains small patches or zones of peloids within micrite, but is primarily equant calcite spar (64%) with moldic to vuggy porosity (14%). This microfacies is associated with a bioherm environment, and based on the lack of bioclasts, the depositional environment of

this microfacies was the backreef lagoonal area. The high amount of equant spar that infilled massive solutional porosity suggest this microfacies underwent major dissolution, most likely in multiple phases.

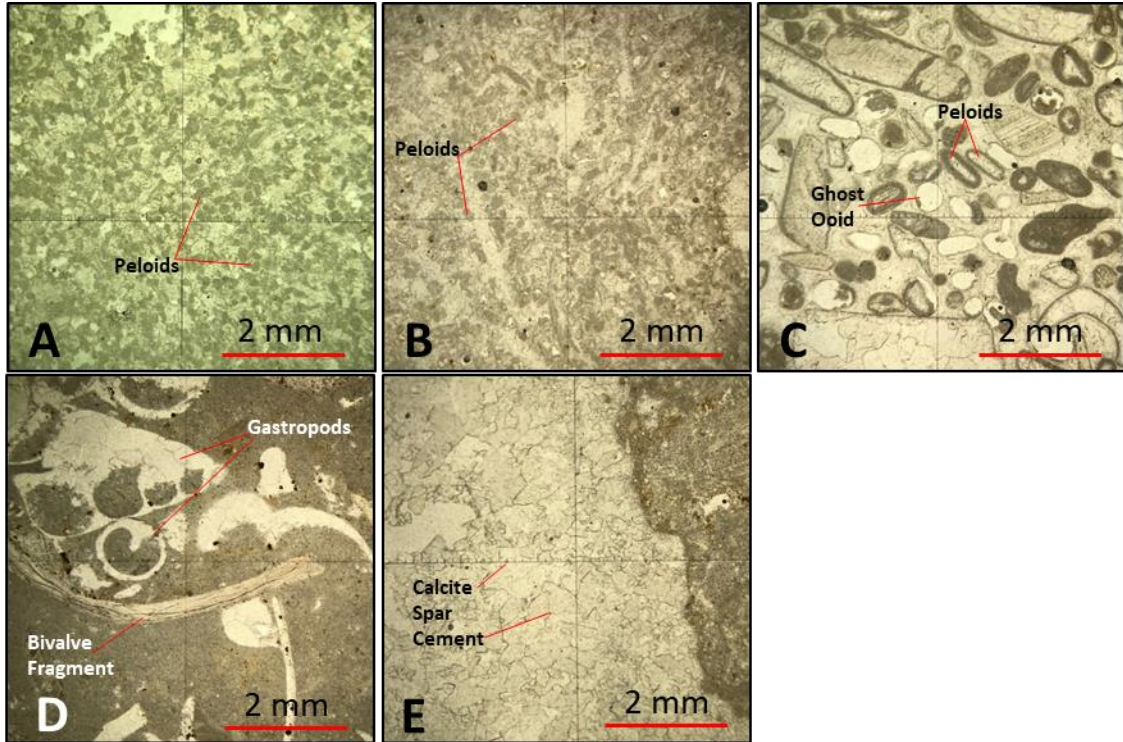


Figure 9: Mobile grain flat facies, all microphotographs are in plane polarize light and viewed at 4x magnification. A) F-3, shows a facies dominated by peloids, with some small bivalve fragments mixed within. B) F-10, shows another facies dominated by peloids, though slightly more bivalve fragments can be seen. C) F-11, shows a peloidal facies that is not as packed and has much more intergranular calcite cement, ghost ooids can also be seen. D) F-7 shows large gastropod and bivalve fragments within a micrite matrix. E) F-5 shows a calcite sparr infill and micritic material.

### Owl Mountain Province Depositional Model

The depositional model for the Owl Mountain Province focuses on the middle shelf environment. Wave approach was from the northeast out of the North Texas-Tyler Basin. Along the shelf margin, the Central Texas reef trend

formed, but the rudist-dominated reefs of the middle shelf were not a continuous barrier reef system like the Stuart City Trend to the southeast (Figure 1). Larger reefs formed to the north and west, but the study area was located on the flank or margin of the main reef trend, where reef growth was restricted in shallow waters and lower energy environments (Figure10).

The northeast margin of the study area is composed of elongate and smaller lobate bioherms dominated by rudist bivalves, in association with algae, bryozoan, foramifera, and others. The elongate reefs formed farther from shore and acted as a protective barrier for the lobate bioherms behind them; this relationship shielded the lobate bioherms from incoming ocean waves. In between these reef trends, channels formed and transported sediment farther inland. Behind and amongst the bioherms were the mobile grain flat associated microfacies, which are composed primarily of ooids and peloids with other bioclasts. These microfacies would migrate along the flanks of the bioherms, becoming more sorted towards the channels. Moving farther inland, the mobile grain flats graded into the peritidal mud flat microfacies, with calmer conditions and shallower water depths; the fossils present in these microfacies are generally intact within a clean micrite matrix. These areas together make up the middle shelf environment of the Owl Mountain Province, though sea level changes would have an effect on deposition. As sea level rose, the middle shelf would migrate shoreward and the patch reefs would grow with sea level. As sea level fell, the middle shelf would migrate offshore towards the basin, and the bioherm

growth would be terminated and covered with the mud flat microfacies as the area transitioned from subtidal to peritidal. These transgressive/regressive sequences would cause the depositional environment to migrate, as expressed in the vertical sections in the study area.

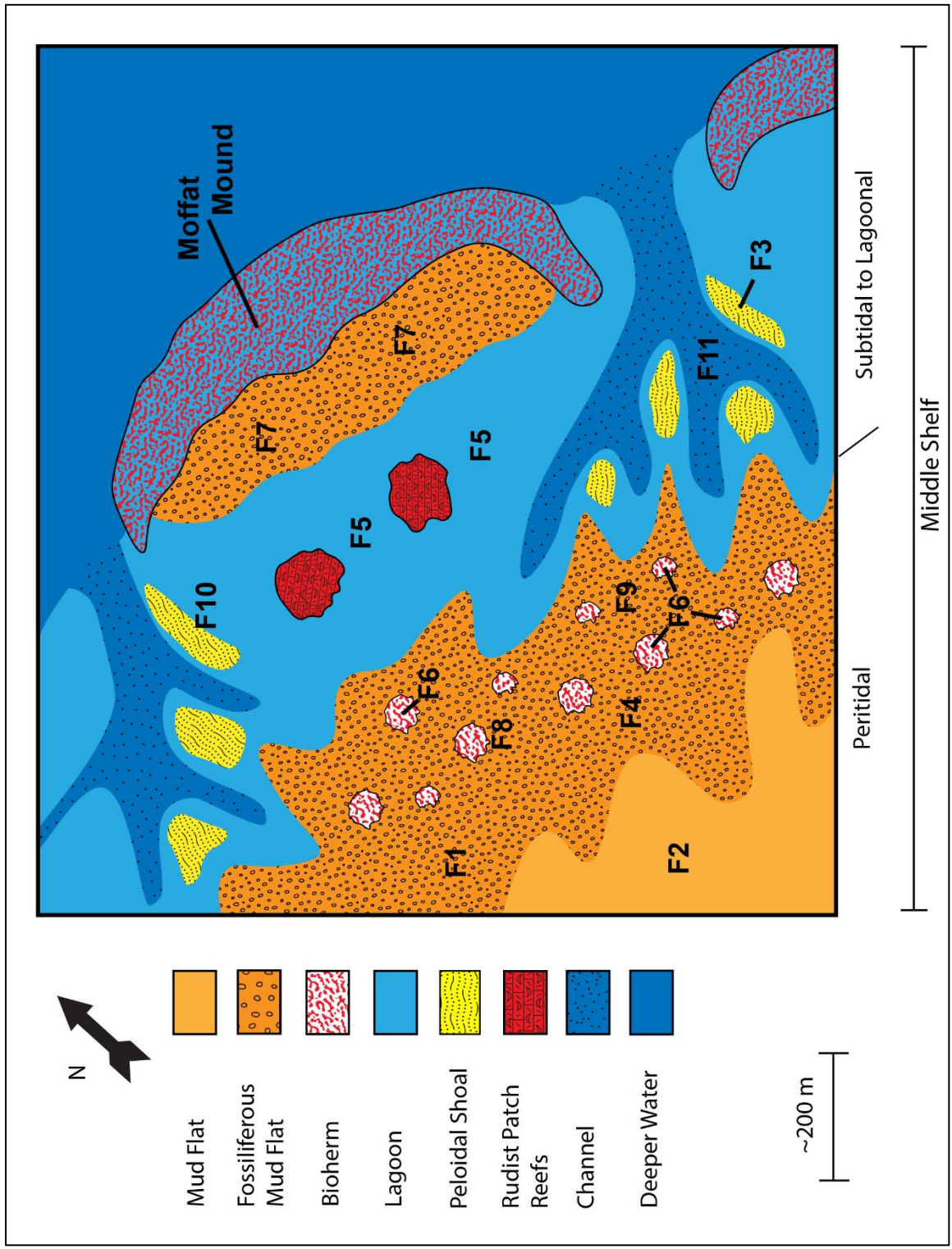


Figure 10: Depositional model for the Owl Mountain Province showing microfacies locations. Microfacies designations are made in Table 1.

Table 1: List of microfacies depicted in the depositional model for the Owl Mountain Province.

<b><u>Microfacies Identified in the Owl Mountain Province</u></b>	
<u>Shallow Peritidal</u>	<u>Shallow Subtidal</u>
F1: Sparse Bioclastic Mud Flat	F3: Peloidal Shoal
F2: Dolomite Mud Flat	F5: Sheltered Bioclastic Lagoon
F4: Bivalve Mud Flat	F6: Bivalve Bioherm
F7: Gastropod Mud Flat	F8: Bioherm Flank
	F9: Inter-biohermal Channel
	F10: Sheltered, Peloidal Backreef/Bioherm
	F11: Channelized Peloid

Seven measured sections along a southwest-northeast trend (Figure 11) were used to create a theoretical cross section (Figure 12) of the depositional environments in the study area. This theoretical model assumes the continuity of microfacies between measured sections due to limited field access to measurable outcrops. There are some areas where visual inspection of potential microfacies is impossible; the area is a heavily vegetated plateau and the vertical profile of areas not visible or accessible can only be inferred. The trend of this section is ideal for the development of the depositional model of the Owl Mountain Province, as it provides substantial evidence of the middle shelf environment present on the Comanche Shelf in the Lower Cretaceous.

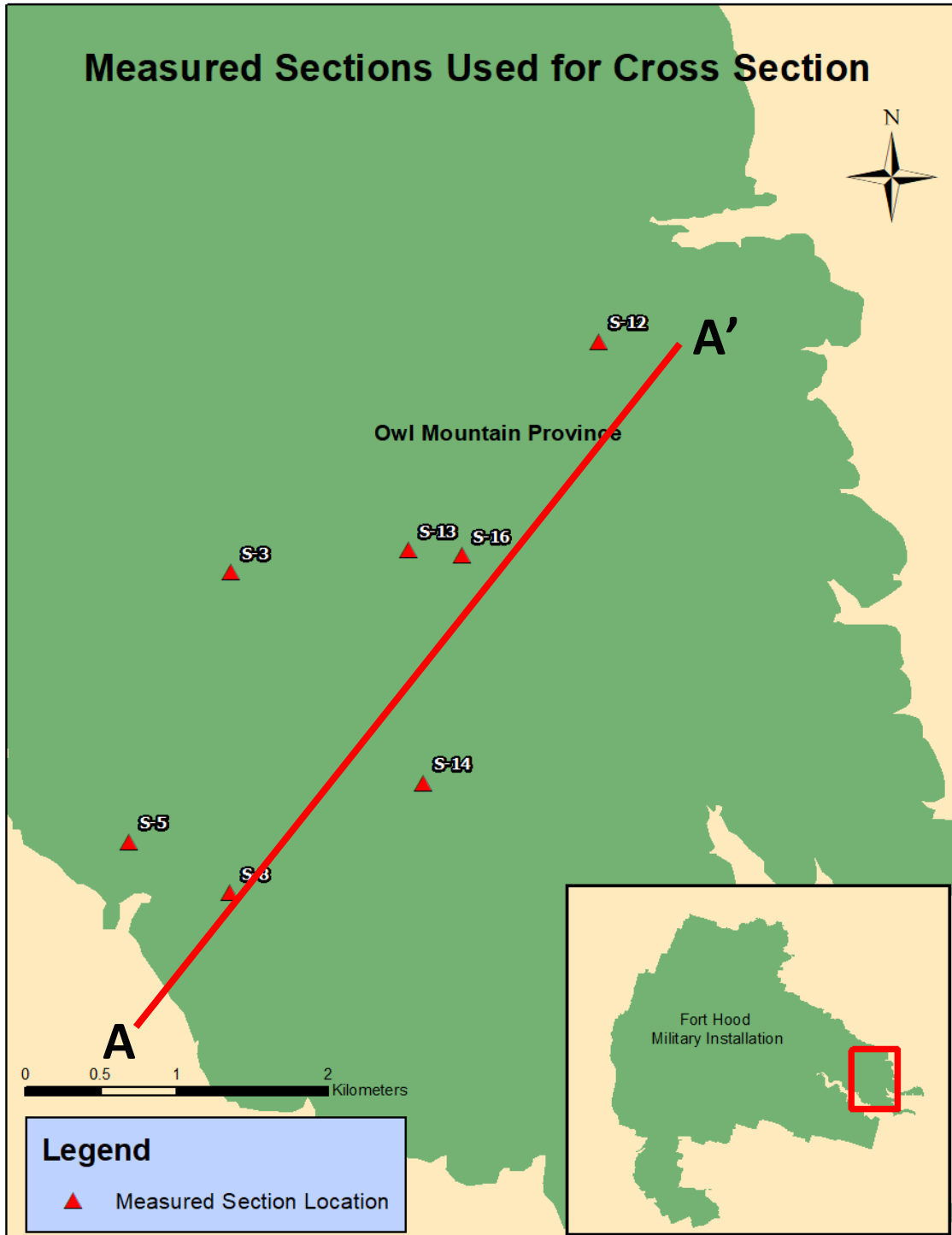


Figure 11: Map showing the measured sections that were used to construct the A – A' cross section.

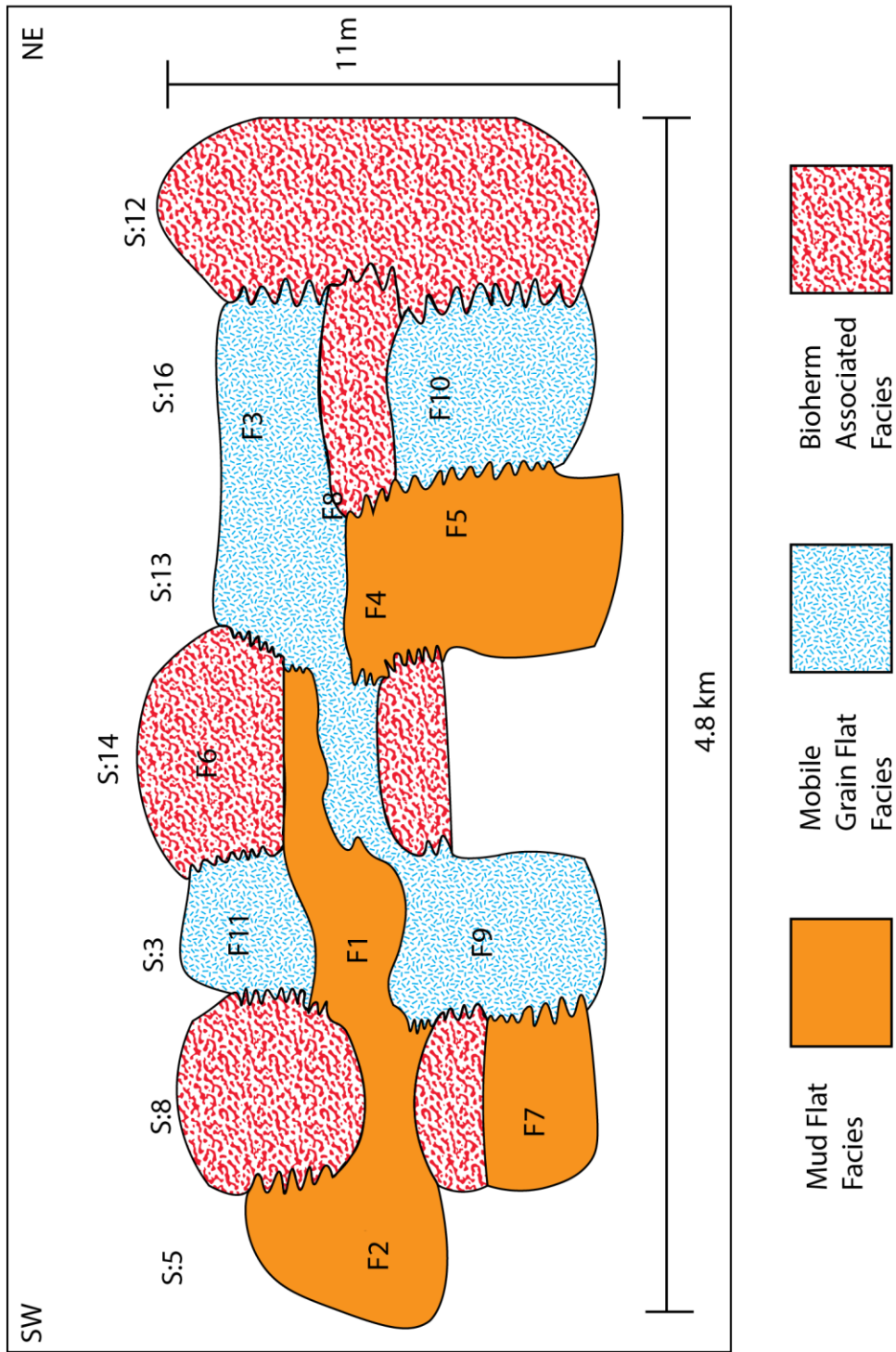


Figure 12: Theoretical cross section showing the facies associations in the study area.

The theoretical cross section shows a relationship between three different facies associations: the mud flat facies, mobile grain flat facies, and the bioherm associated facies. The location of the facies relative to one another portrays the transitional nature of the associations seen in the depositional model, the mud flat facies is shoreward from the mobile grain flat facies, which is then shoreward and adjacent to the bioherm associated facies. This pattern is seen vertically staggered, moving up and also basinward or shoreward, which is indicative of the transgressive/regressive cycles that generated these strata.

### **Diagenetic Model**

A diagenetic model (Figure 13) was created using data gathered from thin section analyses, and the diagenetic history created for each thin section. These individual histories were combined into an overall 18-phase model that represents the diagenetic evolution of the strata in the study area. Some samples provide evidence of each phase of the entire model while others represent some or most of the phases. The model shows 16 phases because neomorphism had two occurrences (aragonite and calcite) and two phases of de-dolomitization are thought to have occurred. The model exhibits multiple phases that occurred beginning with deposition and eogenetic events, mesogenetic events, and lastly telogenetic events which continue to present day.

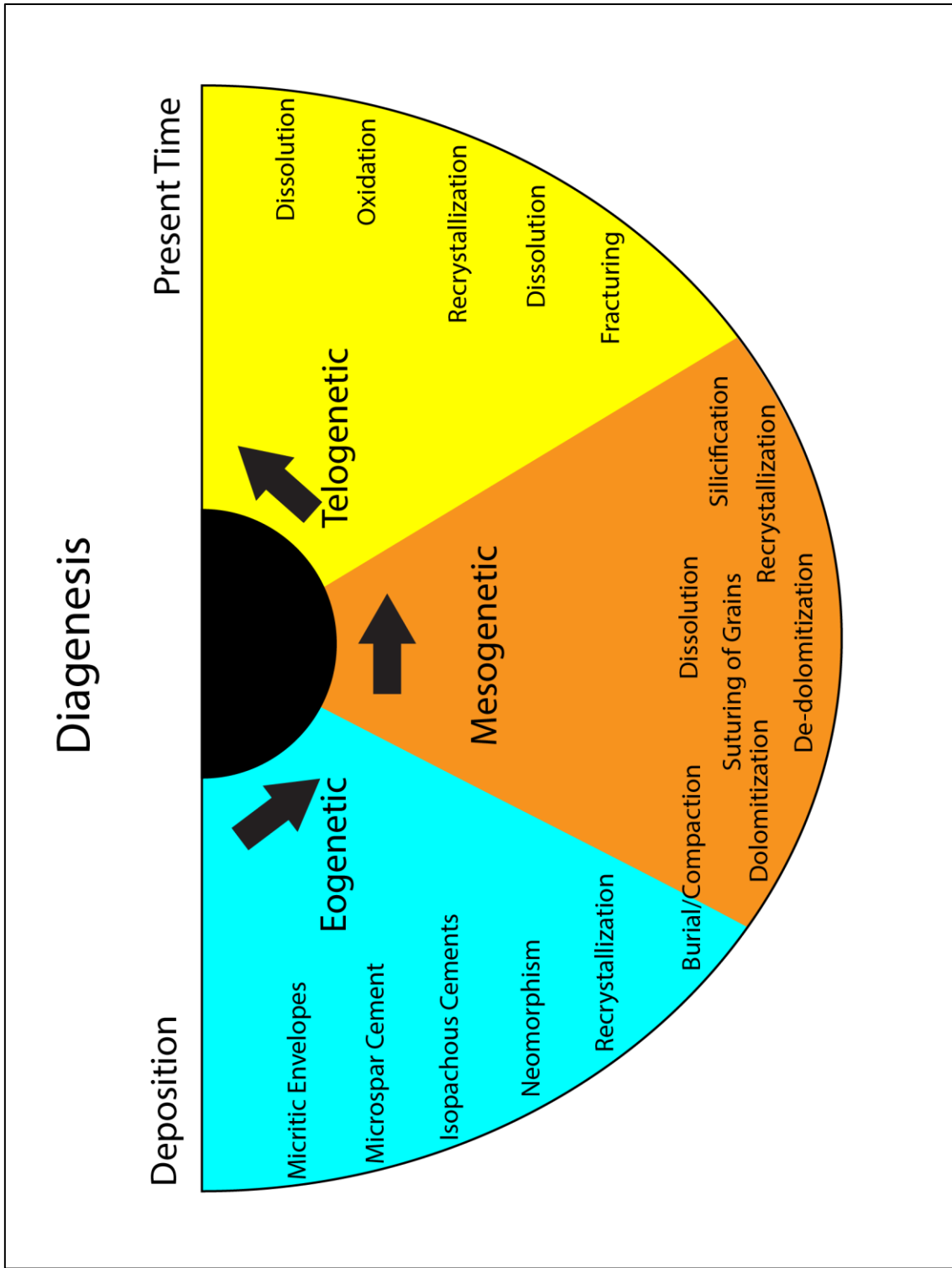


Figure 13: Diagenesis model showing timeline from deposition to present time with diagenetic features listed.

## Eogenetic

The early diagenetic events are syndepositional, after deposition, the precipitation of microspar calcite along the rims occurred contemporaneously with micritic envelopes, soon followed by the development of isopachous cements around some of the allochems. These events occurred before significant burial of sediments. The next phase would include neomorphism of aragonite to low-Mg calcite as well as recrystallization of some aphanocrystalline calcite cements to equant spar cements. It is unclear whether the first stage of dolomitization occurred at this time or soon after burial. Microfacies F-2 shows evidence of early dolomitization and microfacies F-9 shows evidence of later stage dolomitization, so it is possible that some microfacies underwent one or the other, or both.

## Mesogenetic

During mesogenetic diagenesis, burial and compaction began, though the lack of deep burial features suggests that burial was shallow for an extended amount of time. Porosity inversion involving the dissolution of some allochems and recrystallization into intergranular equant calcite spar occurred.

Dolomitization also occurred around this time (Fisher and Rodda 1969), with some allochems infilled by calcite cements. As the burial depth increased, dedolomitization occurred, leaving some ghost allochems that were filled with

calcite spar cement. A second phase of dolomitization occurred during this stage, which is seen in microfacies F-11. Silicification also occurred at this time, and is hypothesized to be hydrothermal in nature associated with Late Cretaceous volcanism occurring near the study area (Rose, 2016; Ewing, 1991). The silica in microfacies F-9 occurs as opal and as mega quartz; the opal is generally replacing dolomite or calcite within the allochems, and the mega quartz is generally infilling pore spaces.

### Telogenetic

Uplift/exhumation of the strata resulted in brittle deformation, which formed pathways for fluid migration, eventually causing more dissolution and recrystallization as the strata moved into the shallow phreatic zone. Oxidation of some allochems and grains also begins to occur in this stage and continues as the strata are exposed. The study area has undergone significant dissolution from exposure to present time, causing vuggy porosity and giving rise to the karst features such as sinkholes and caves in the Edwards limestone. As fluids continue to migrate through the strata, more dissolution is occurring during present time.

## Conclusions

The delineation of heterogeneous carbonate strata, including detailed mapping and petrographic analyses, have helped provide valuable insight into the depositional and diagenetic history of the unique microfacies associated with the Owl Mountain Province within the Fort Hood Military Installation. The 11 microfacies described are associated with middle shelf sub-environments including mud flats, mobile grain flats and bioherm facies. The patch reefs built by rudist bivalves were smaller than those that made up the bulk of the Central Texas Reef Trend because they formed on the southern margin of the trend across the flank of the Belton High. The mobile grain flats were composed of ooids and peloids as well as bioclasts shed from the patch reefs. This group was migratory and controlled by the oscillating current between the patch reefs. Shoreward, the environment was calmer and graded into the peritidal mud flat environment where deposition was tidal controlled with influence by storm events. It was most likely in this environment where some supratidal influence was exerted as evidenced by the presence of dolomite in those microfacies. These unique environments were protected from oceanic wave energy by the larger Central Texas Reef Trend to the north and by the Stuart City Trend to the southeast. These microfacies were directly controlled by sea level rise and fall, as patch reefs could only grow vertically in response to sea level changes. Transgressive and regressive periods provided the mechanism for the migration

of this environment basinward and shoreward across the area until deposition terminated.

The microfacies in this study underwent a complex diagenetic history, with 18 phases of diagenesis determined through petrographic analyses. These included eogenetic events, such as marine cements, neomorphism, and dolomitization. Mesogenetic events included burial/compaction, recrystallization, dissolution, as well as a second phase of dolomitization. The dolomitization is postulated to be via seepage-reflux, following the model developed by Fisher and Rodda (1969), or possibly related to hydrothermal events. Silicification occurred at the end of the mesogenetic phase of diagenesis, which may have been related to Late Cretaceous volcanism (Rose, 2016; Ewing, 1991). Telogenetic events included fracturing, dissolution, recrystallization, oxidation, and eventually karst manifestation.

The microfacies determined in this model followed a similar assemblage to the model developed by Kerr (1977), though they do not include some of the microfacies in his model. Kerr's model focused on the Belton area and depicts inner and middle shelf environments, whereas the Owl Mountain Province model only depicts middle shelf environments with possible influence by inner shelf processes. Brown's research (1975) described more complex depositional environments, including beach microfacies, open shallow marine, supratidal, and an open shelf environments. Moffatt Mound was a fairly large mound structure which would have created its own unique environments that differ from the Owl

Mountain Province. Amsbury's model (1984) focused on Moffatt Mound which is proximal to the study area and likely influenced the study area. Microfacies analyses and field evidence from this study does not support many of the environments proposed by these previous works. It is possible that Moffatt Mound actually exerted some influence on this study area, providing protection and shedding sediments that would eventually migrate into this area and be incorporated into the Lower Cretaceous strata found in the Owl Mountain Province.

## REFERENCES

- Amsbury, D.L., T.A. Jr. Bay, and F.E. Lozo. "A Field Guide to Lower Cretaceous Carbonate Strata in the Moffatt Mound Area near Lake Belton, Bell County, Texas." *Guidebook for SEPM Field Trip NO. 3*. San Antonio: Gulf Coast Section of the Society of Economic Paleontologists and Mineralogists Foundation, 1984. 1-19.
- Bebout, D.G., and Loucks, R.G., 1977, Cretaceous carbonates of Texas and Mexico: applications to subsurface exploration: University of Texas Bureau of Economic Geology Report of Investigations, no. 89, 346 p.
- Brown, J L. *Paleoenvironment and Diagenetic History of the Moffat Mound, Edwards Formation, Central Texas*. Master's Thesis, Baton Rouge: Louisiana State University, 1975.
- Bryant, A.W. *Geologic and Hydrogeologic Characterization of Groundwater Resources in the Fredericksburg Group, North Nolan Creek Province, Bell County, Texas*. Master's Thesis, Nacogdoches: Stephen F. Austin State University, 2012
- Cannata, S.L., and J.C., Jr. Yelderman. "Hydrogeology of the Edwards Aquifer in the Washita Prairie: Bosque, Coryell, Hamilton and McLennan counties, Texas." *Hydrogeology of the Edwards Aquifer: Northern Balcones and Washita Prairie segments*. Austin: Austin Geological Society, 1987. 47-60.
- Damman, A.J., 2010, *A Comparison of the Cretaceous (Albian) Edwards Limestone Bioherms of Central Texas with the Holocene Coral Reefs of Bermuda* (Masters Thesis). Balyor University.
- Ewing, T. E., 1991, The tectonic framework of Texas: Text to accompany "The Tectonic Map of Texas": Texas Bureau of Economic Geology, Austin, 36 p.
- Fisher, W.L., and P.U. Rodda. "Edwards Formation (Lower Cretaceous), Texas: Dolomitization in a Carbonate Platform System." *American Association of Petroleum Geologists* 53, no. 1 (1969): 55-72.
- Forbes, K.A., 2011, Bermuda's Climate and Weather: Year-round temperatures and hurricanes, cooler in winter than Caribbean 1,000 miles south: Bermuda Online, [www.bermuda-online.org/climateweather.htm](http://www.bermuda-online.org/climateweather.htm)

- Forster, A., Schouten, S., Baas, M., and Sinnenhe Damsté, J.S., 2007, Mid-Cretaceous (Albian-Santonian) sea surface temperature record of the tropical Atlantic Ocean: *Geology*, v. 35, no. 10, p. 919-922.
- Jacka, A.D., and Brand, J.P., 1977, Biofacies and development and differential occlusion of porosity in a Lower Cretaceous (Edwards) reef: *Journal of Sedimentary Petrology*, v. 37, no. 1, p. 366-381.
- Kerr, R. S., 1977, Development and diagenesis of a Lower Cretaceous bank complex, Edwards Limestone, north central Texas, *in* D. Bebout and L. Loucks, eds., *Cretaceous carbonates of Texas and Mexico*: Austin, Texas., Bureau of Economic Geology, p. 216-233.
- Nelson, H.F. "The Edwards Reef Complex and Associated Sedimentation." *The Geological Society of America*. Dallas: Bureau of Economic Geology, 1973. 1-35.
- Plumley, W.J., Risley, G.A., Graves, R.W. Jr., Kaley, M.E., 1962, Energy spectrum of carbonate rocks – A Symposium: American Association of Petroleum Geologists. Mem. 1, p. 85-107.
- Roberson, D.S., 1972, The Paleocology, Distribution, and Significance of Circular Edwards Limestone Bioherms in Central Texas [Master's Thesis]: Baylor University, 80 p.
- Rose, P.R. *Edwards Group, Surface and Subsurface, Central Texas, Report of Investigations*. Austin: Bureau of Economic Geology, 1972, 198.
- Rose, P. R., "Late Cretaceous and Tertiary Burial History." *Gulf Coast Association of Geological Societies*. v. 5 (2016): p. 141-179.
- Scott, R.W., 1990(a), Models and stratigraphy of Mid-Cretaceous reef communities, Gulf of Mexico: *SEPM Concepts in Sedimentology and Paleontology*, v. 2, 102 p.
- Steuber, T., Rauch, M., Masse, J.-P., Graaf, J., and Malkoč, M., 2005, Low-latitude seasonality of Cretaceous temperatures in warm and cold episodes: *Nature*, v. 437, no. 27, p. 1341-1344.
- Wilson, P.A., and Norris, R.D., 2001, Warm tropical ocean surface and global anoxia during the mid-Cretaceous period: *Nature*, v. 412, p. 425-429.

Young, K.P., 1959, Edwards fossils as depth indicators *in* Symposium on Edwards Limestone in Central Texas: University of Texas Bulletin, 5905, p. 95-104.

## **APPENDIX A: EXTENDED PREVIOUS WORKS**

### **Previous Models**

The Edwards Limestone of the Lower Cretaceous spans across a vast majority of Central Texas. The Stuart City Trend formed a barrier reef along the shoreline of the ancestral Gulf of Mexico which provided protection from ocean waves (Roberson, 1972). Behind the Stuart City Trend, the Edwards Limestone, regionally considered a backreef facies (Roberson, 1972), was deposited on the Comanche Shelf, this area is also referred to as the Central Texas Reef Trend. The shelf provided a stable, protected environment for smaller, more numerous patch reefs to form, these patch reefs formed as elongate and circular reefs (Roberson, 1972; Damman, 2011). This area of biohermal mounds and patch reefs was bounded on the north, northeast, and south by basins of deeper water, and to the west by the Llano uplift and Kirschberg Lagoon. Kerr (1977), developed a model for the greater Belton, Texas area that showed these features; the model shows the progradation of inner and middle shelf facies as sea level fell (figure A-1).

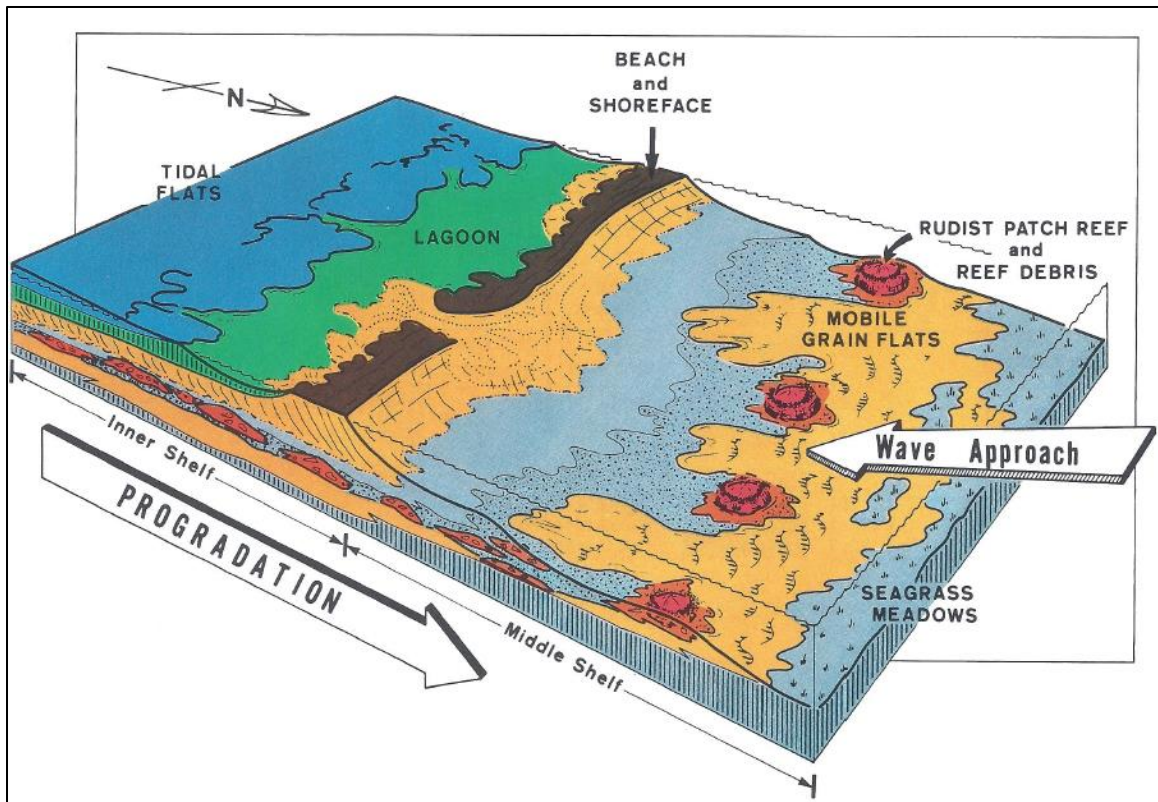


Figure A-1: Depositional model of the Edwards Limestone in the area of Belton, Texas, shows progradational inner and middle shelf facies (from Kerr, 1977).

Previous works show that the environment of deposition was calm to agitated, evidenced by the dominant rock type of micrite or fine carbonate mudstone (Roberson, 1972; Plumley et. al., 1962). The mostly intact nature of the fossils and presence of fecal pellets within the reef rock also suggest a calm environment. Swale and ripple marks suggest wave action over the reef area, ammonite casts among the reef rock also suggest currents or waves strong enough to transport large shells (Roberson, 1972). The combination of the low energy to slightly agitated environments allowed the deposition of the Edwards Limestone within the study area. The water temperature of the environment was

warm, thought to be the warmest part of the Cretaceous, with temperatures calculated to be between 32-34°C, possibly higher, with waters warm year round (Damman, 2010; Forster, 2007; Steuber et al., 2005; Wilson and Norris, 2001;). The lack of corals present during this time also suggests that the temperatures were warmer than 30°C, though they are more abundant to the southeast towards deeper waters (Damman, 2010p; Scott, 1990a). The rudist reefs of Central Texas exhibit low biodiversity, with only 18 species of rudist identified, compared to the 792 total species identified in the Middle East and Mediterranean (Damman, 2010; Steuber, 1999). Other than rudists, only a few species of echinoderms, bivalves, gastropods, bryozoans, foraminifera, and algae are found (Damman, 2010). The salinity of the waters was fairly high, even hypersaline at times, with an average salinity of 36.2-36.6 parts per thousand. The saline conditions and warm water temperatures led to the low biodiversity of the reefs, with rudists being able to withstand harsher conditions than the corals, this explains why the rudists thrived during this time as oppose to the corals. The deposition of the Edwards reef limestone was controlled by sea level, the reef growth was directly dependent on water level (Roberson, 1972; Damman, 2010). The bioherms in the area were measured to be between 10-100m in diameter, with a height not to exceed the estimated water depths of 7-8m (Damman, 2010; Bedout and Loucks, 1974; Young, 1959). As sea level dropped, Jacka and Brand, (1977) proposed that the Edwards Limestone was sub-aerially exposed up to 40m; oxidation, case hardening, borings, and the presence of terra rossa

soils at the top of the Edwards are evidence of this environment. The Kiamichi shale formation onlaps the Edwards Formation unconformably, though the Kiamichi may not be present over some of the patch reefs due to variable relief provided by the Belton High (Nelson, 1959).

Damman (2011), compared the patch reefs of central Texas to the modern Bermuda coral reefs. Many factors of each reef system were similar, including climate, salinity, energy, turbidity, current, reef shapes, bioherm sizes, reef depth, reef protection, biodiversity, zonation factors, and grain size (Damman, 2011). The only key difference between the two reef environments was water temperature. The Bermuda reefs are considered to be “cold water” reefs with winter temperatures on the outer reefs falling to as low as 18° C; though for much of the year they are warmer at 25° to 28° C (Forbes, 2011; Damman, 2010).

The formations in the study area follow a trend that is thought to be a mound structure, which can be modeled after Moffatt Mound (figure A-2) (Cannata and Yelderman 1987; Amsbury et al. 1984; Brown 1975), also referred to as the Moffat Lentil in other literature (Rose 1972). The mound is described as a lenticular, abnormally thick part of the Edwards that consists of oolite and pellet rocks, in contrast with the rudist limestone, miliolid wackestone and grainstone, chert, and secondary rock types characteristic of the Edwards elsewhere (Amsbury et al. 1984).

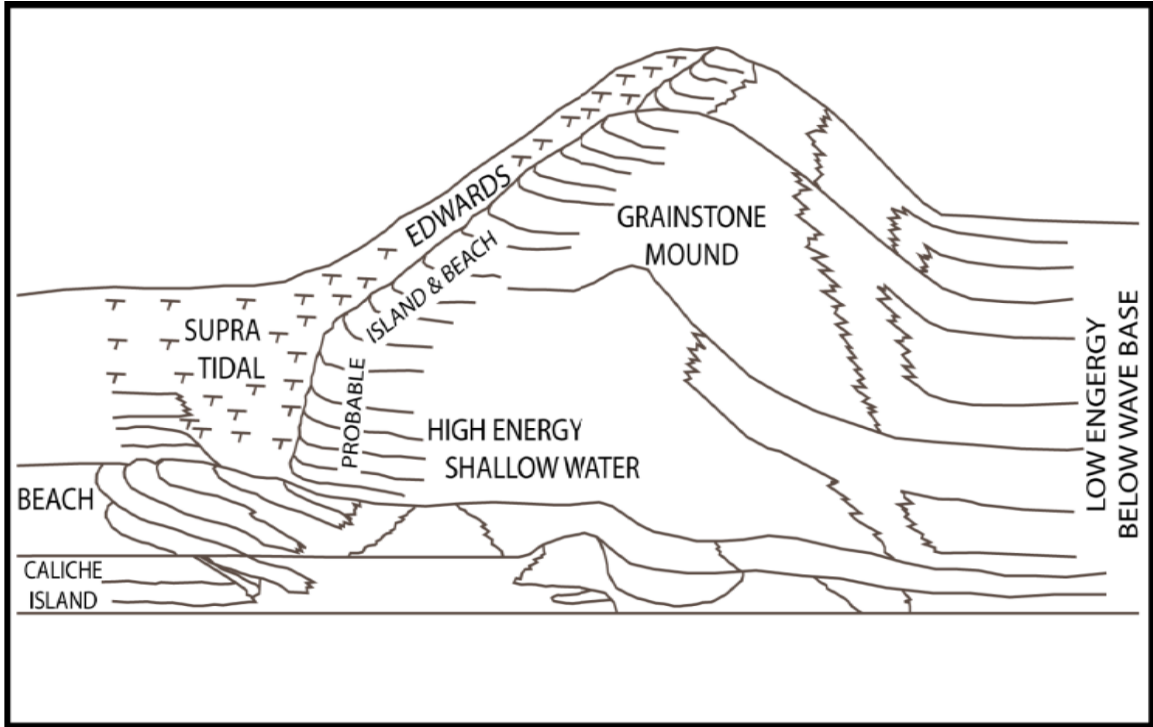


Figure A-2: Conceptual model of mound structure with facies development, (from Byrant 2012; modified from Amsbury et al. 1984).

The Moffatt Mound trend and strata from the study area are structurally similar, and although the Moffatt Mound area consists of thicker, more well-defined outcrops of Edwards strata, they both are lithologically distinct from the main Edwards reef trend. Both the Moffatt Mound trend and strata in the study area formed across the Belton High (Brown 1975). The Moffatt Mound trend formed on or near the axis of the Belton High, whereas Edwards Group strata in the study area were deposited along the lower flanks, to the west in more restricted circulation waters. The primary difference between the two areas is

water depth due to the spatial distribution across the Belton High which influenced the difference in lithology (Brown 1975). The study area, on the western flank of the Belton High, formed in slightly deeper water than the Moffatt Mound facies, which supported different marine life and gentle transitions between depositional environments.

Dolomite in the area has been explained by Fisher and Rodda (1969), with the seepage-reflux model (figure A-3). They postulated that saline brines from the evaporite Kirschberg Lagoon migrated through porous strata such as beach sands and into the Fredericksburg Group (Fisher and Rodda, 1969).

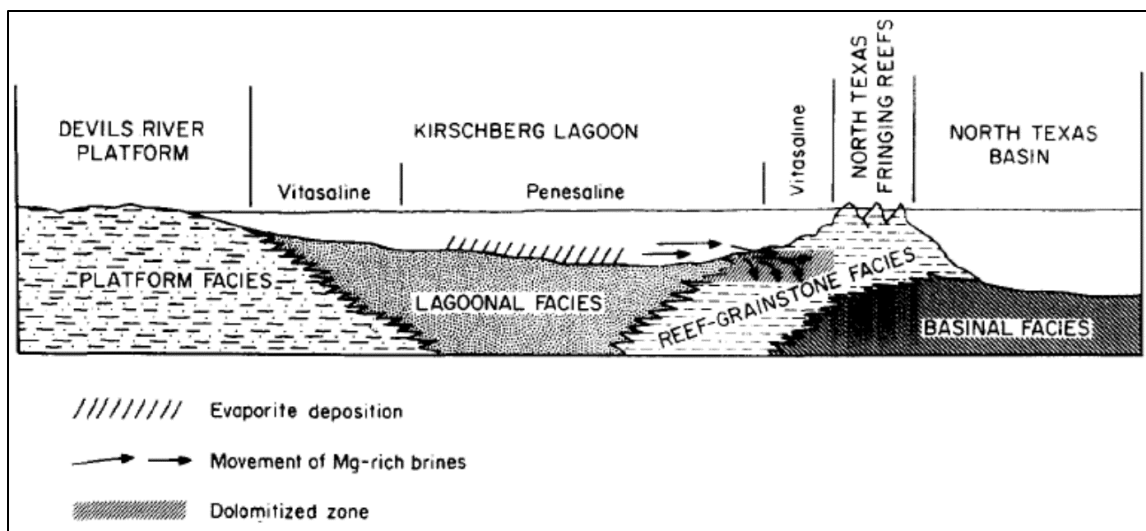


Figure A-3: seepage-reflux model for dolomitization (from Fisher and Rodda, 1969)

## **APPENDIX B: MEASURED FACIES SECTIONS**

### **Introduction**

A total of 16 sections were measured to identify microfacies changes both vertically and laterally across the study area. Sections were measured along road cuts, escarpments, and areas where rock in place was accessible. The sections were measured using traditional outcrop measurement methods, with a metric tape and yellow notebook to record notes and descriptions. For each microfacies established, a sample was thoroughly described in the field, noting the Dunham classification, fresh color, weathered color, iron oxide content, unique minerals seen, primary allochems, clay content, bedding, profile, sedimentary structures, and thickness. Microfacies section 6 is not included in this work due to the samples being rendered unusable in preparation. A microfacies column for each section was also drafted in the field in a notebook for later use; anything found to be helpful or interesting was photographed and/or sketched. At each section, GPS location was recorded using a Garmin Rhino 650, this data was entered into ArcGIS in order to draft location maps.

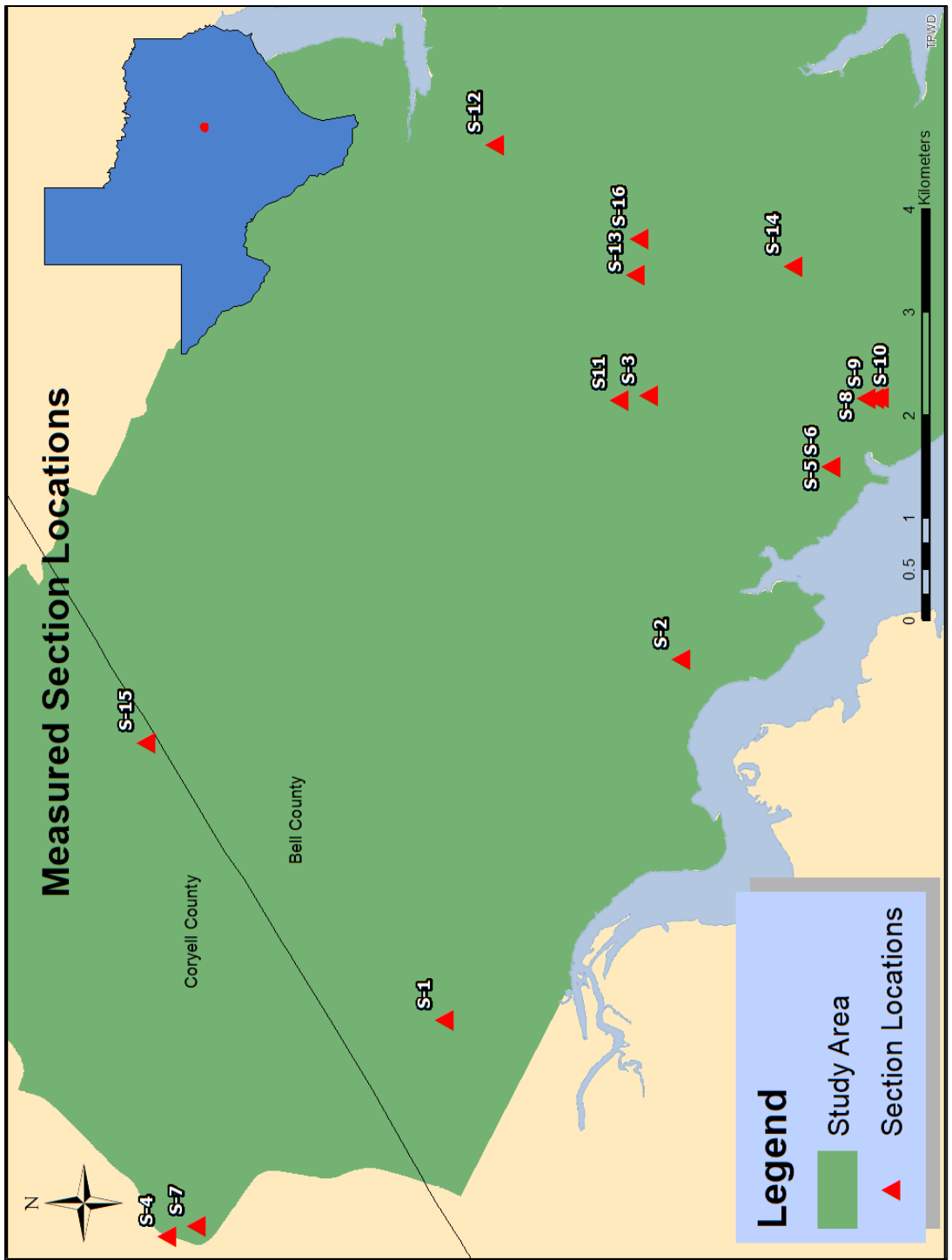
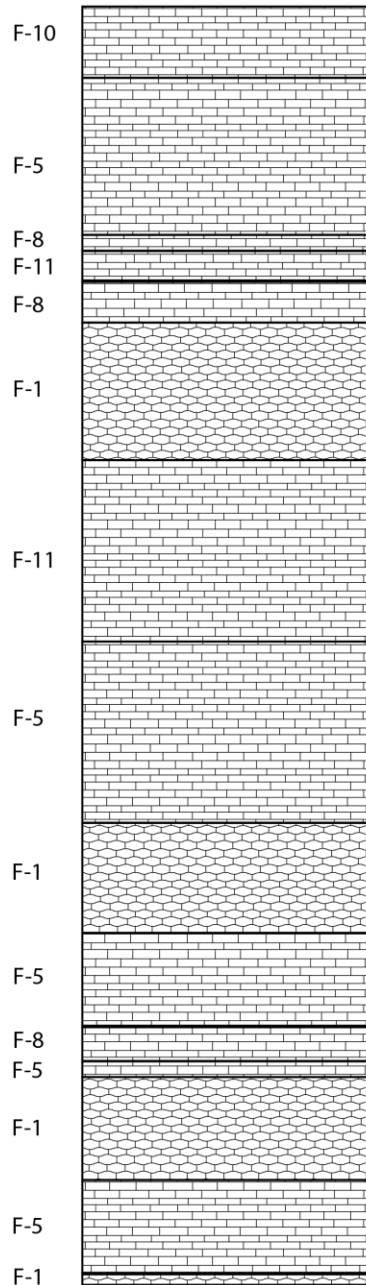


Figure 1: Map showing Owl Mountain Province with measured section locations marked. Source: ArcGIS online database.

### MEASURED SECTION 1



- F-1: Sparse Biomicrite
- F-2: Unsorted Biosparite (Dolostone)
- F-3: Unsorted Pelsparite
- F-4: Sparse Biomicrite
- F-5: Unsorted Pelsparite
- F-6: Unsorted Biosparite
- F-7: Sparse Biomicrite
- F-8: Unsorted Pelsparite
- F-9: Sorted Biosparite
- F-10: Unsorted Pelsparite
- F-11: Sorted Pelsparite

Total thickness of section: 16.3 meters. Measured on January 26, 2016 by Jacob Meinerts and Dr. Mindy Faulkner

Figure 2: Column of measured section 1 with microfacies labels.

## MEASURED SECTION 2

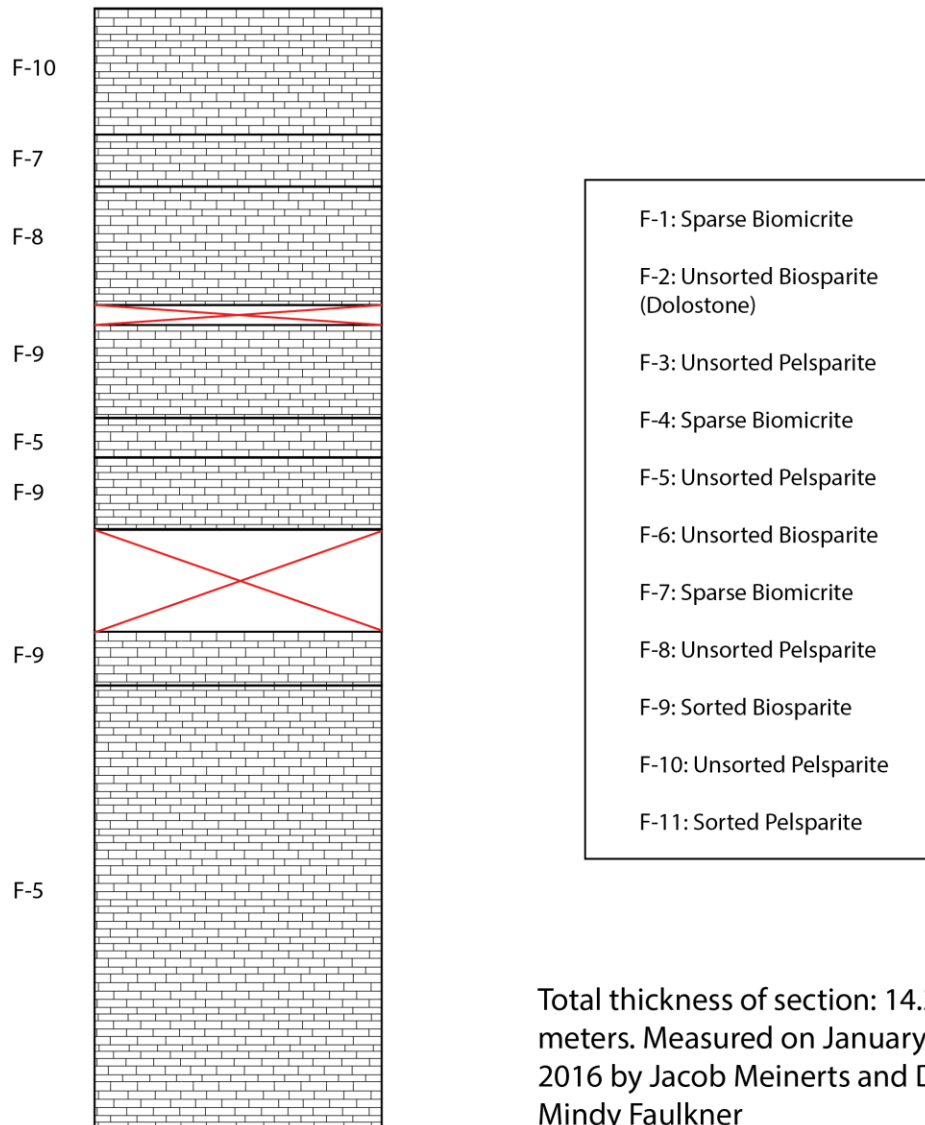
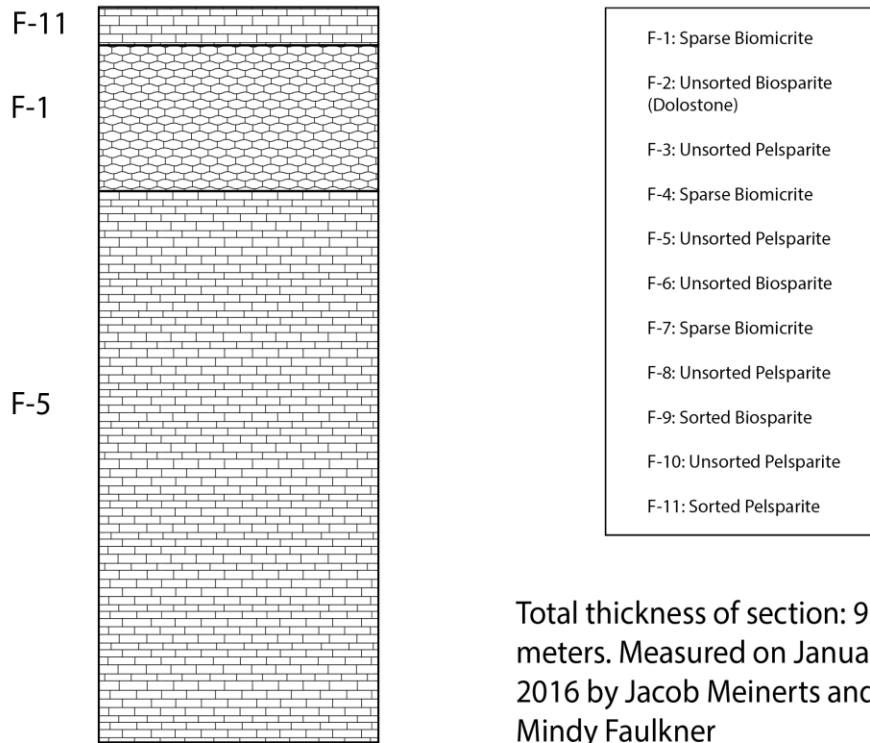


Figure 3: Column of measured section 2 with microfacies labels

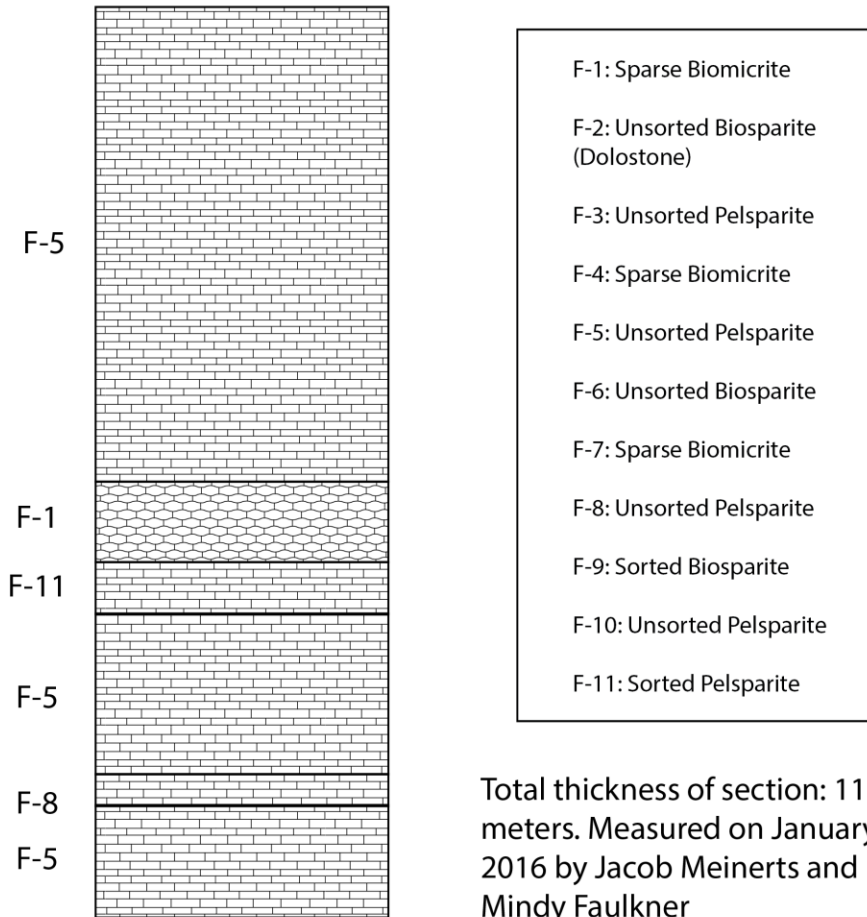
### MEASURED SECTION 3



Total thickness of section: 9.08 meters. Measured on January 28, 2016 by Jacob Meinerts and Dr. Mindy Faulkner

Figure 4: Column of measured section 3 with microfacies labels.

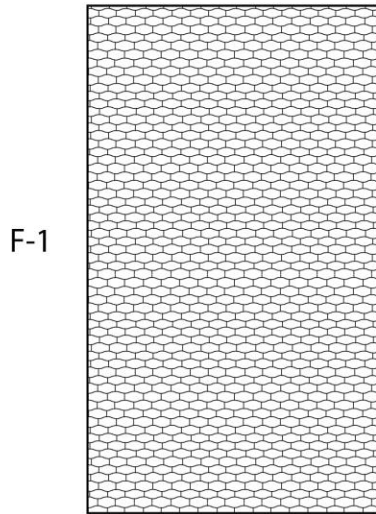
### MEASURED SECTION 4



Total thickness of section: 11.35 meters. Measured on January 28, 2016 by Jacob Meinerts and Dr. Mindy Faulkner

Figure 5: Column of measured section 4 with microfacies labels.

## MEASURED SECTION 5



Total thickness of section: 3.43 meters. Measured on January 28, 2016 by Jacob Meinerts and Dr. Mindy Faulkner

- F-1: Sparse Biomicrite
- F-2: Unsorted Biosparite (Dolostone)
- F-3: Unsorted Pelsparite
- F-4: Sparse Biomicrite
- F-5: Unsorted Pelsparite
- F-6: Unsorted Biosparite
- F-7: Sparse Biomicrite
- F-8: Unsorted Pelsparite
- F-9: Sorted Biosparite
- F-10: Unsorted Pelsparite
- F-11: Sorted Pelsparite

Figure 6: Column of measured section 5 with microfacies labels

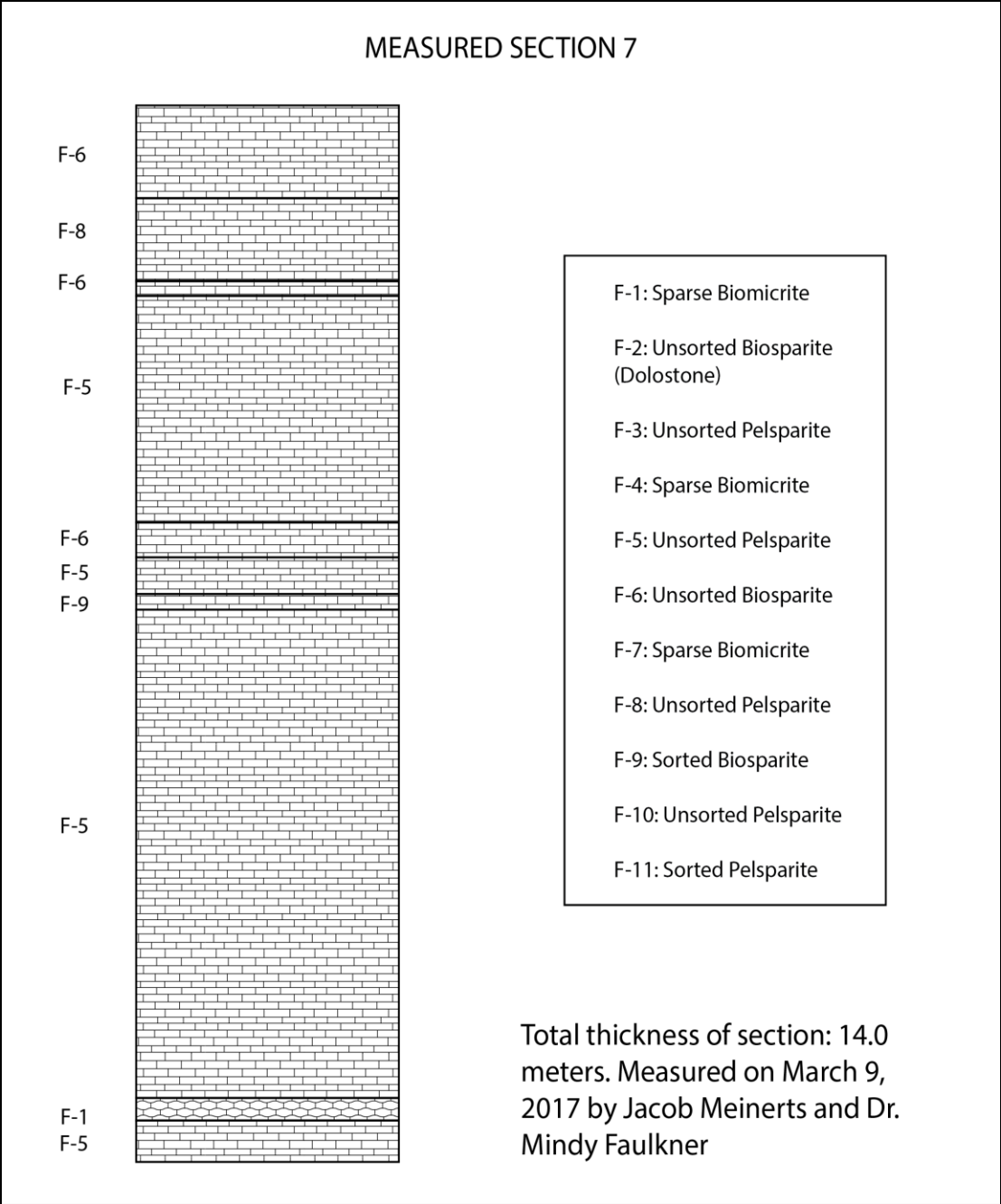


Figure 7: Column of measured section 7 with microfacies labels

### MEASURED SECTION 8

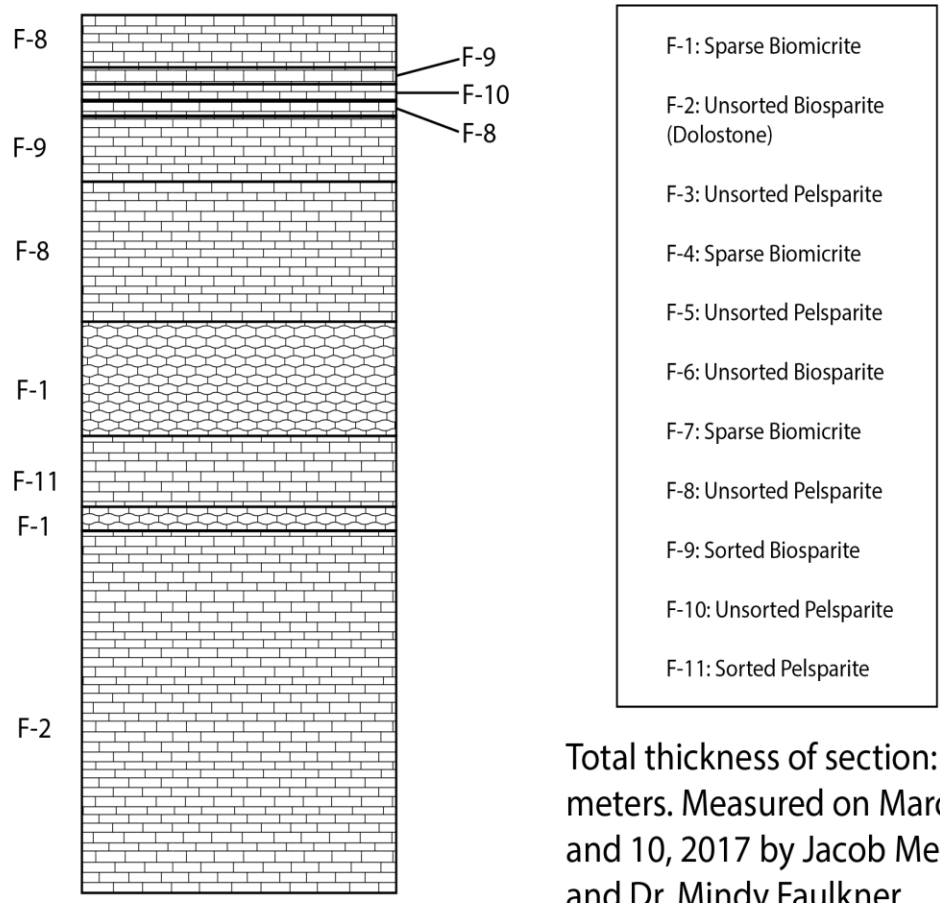
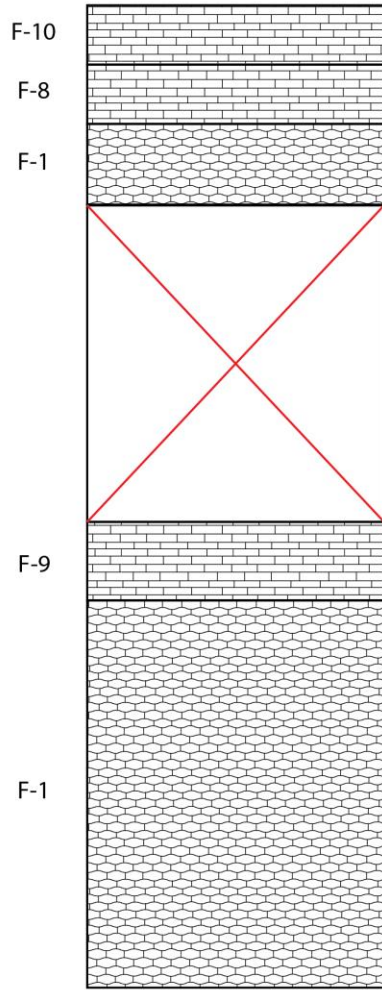


Figure 8: Column of measured section 8 with microfacies labels

### MEASURED SECTION 9

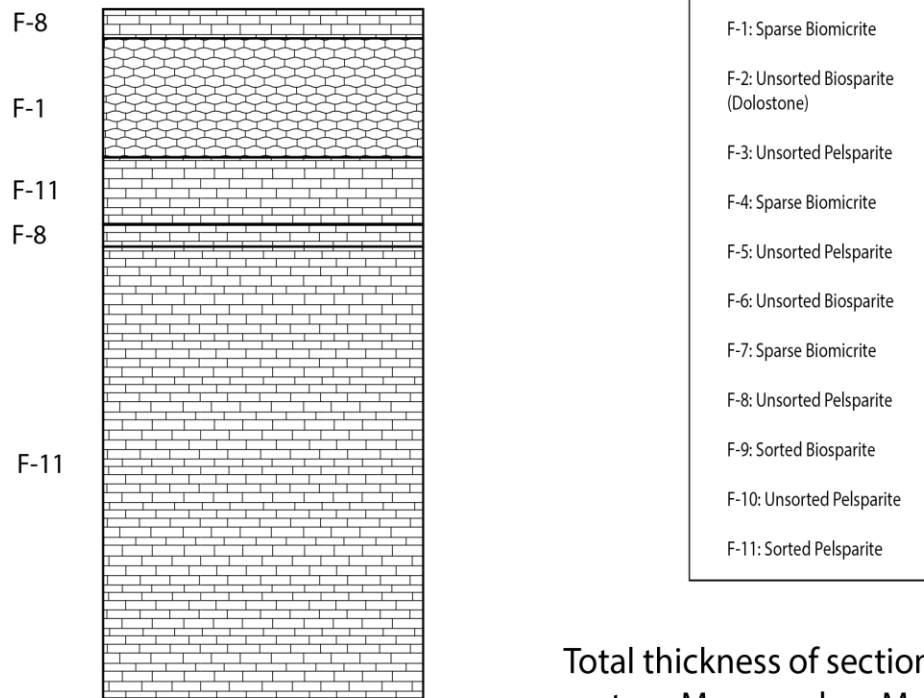


- F-1: Sparse Biomicrite
- F-2: Unsorted Biosparite (Dolostone)
- F-3: Unsorted Pelsparite
- F-4: Sparse Biomicrite
- F-5: Unsorted Pelsparite
- F-6: Unsorted Biosparite
- F-7: Sparse Biomicrite
- F-8: Unsorted Pelsparite
- F-9: Sorted Biosparite
- F-10: Unsorted Pelsparite
- F-11: Sorted Pelsparite

Total thickness of section: 12.13 meters. Measured on March 10, 2017 by Jacob Meinerts and Dr. Mindy Faulkner

Figure 9: Column of measured section 9 with microfacies labels.

## MEASURED SECTION 10



Total thickness of section: 7.5 meters. Measured on March 10, 2017 by Jacob Meinerts and Dr. Mindy Faulkner

Figure 10: Column of measured section 10 with microfacies labels

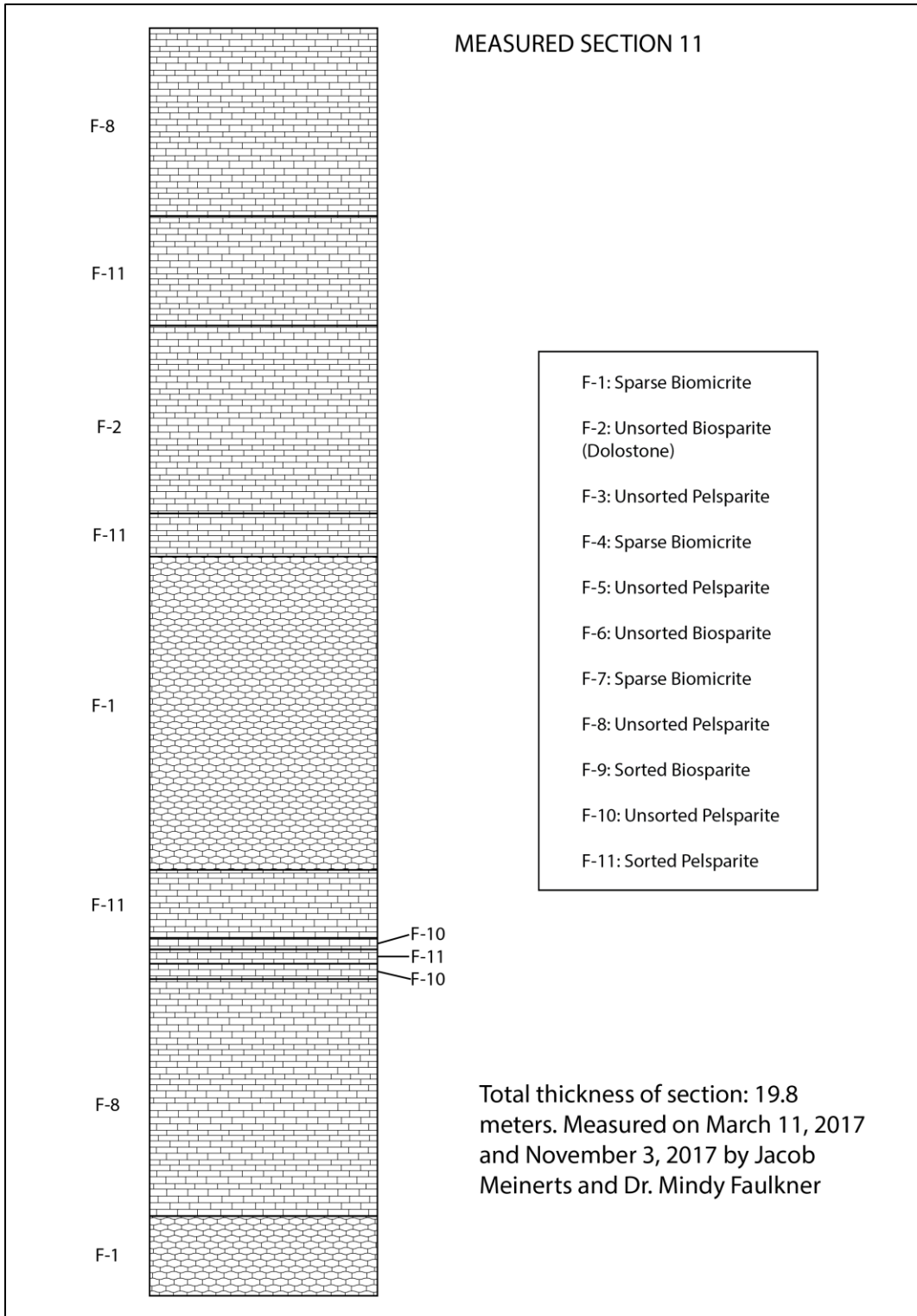
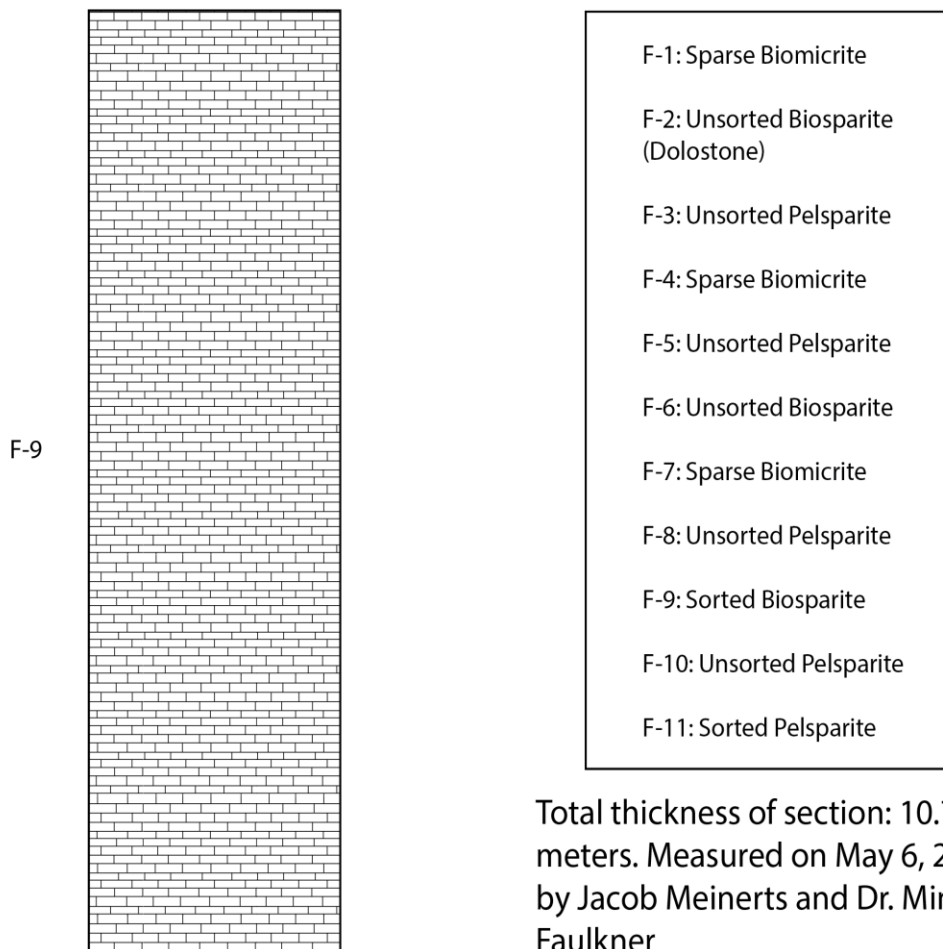


Figure 11: Column of measured section 11 with microfacies labels.

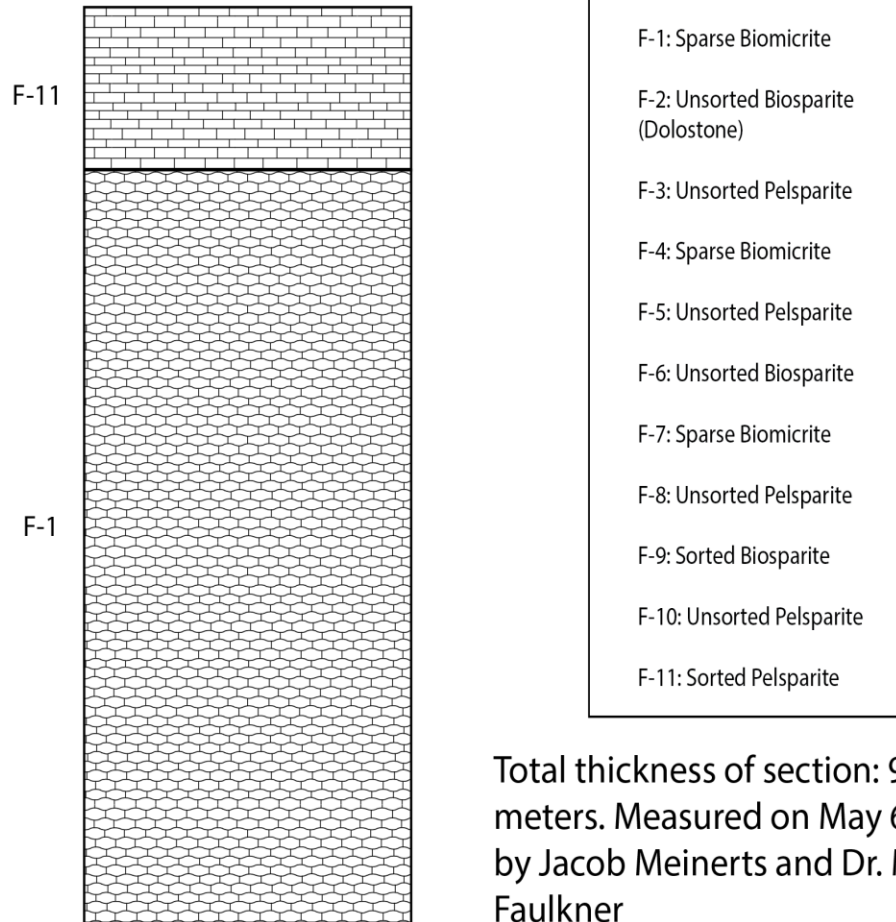
## MEASURED SECTION 12



Total thickness of section: 10.7 meters. Measured on May 6, 2017 by Jacob Meinerts and Dr. Mindy Faulkner

Figure 12: Column of measured section 12 with microfacies labels.

## MEASURED SECTION 13



Total thickness of section: 9.55 meters. Measured on May 6, 2017 by Jacob Meinerts and Dr. Mindy Faulkner

Figure 13: Column of measured section 13 with microfacies labels

## MEASURED SECTION 14

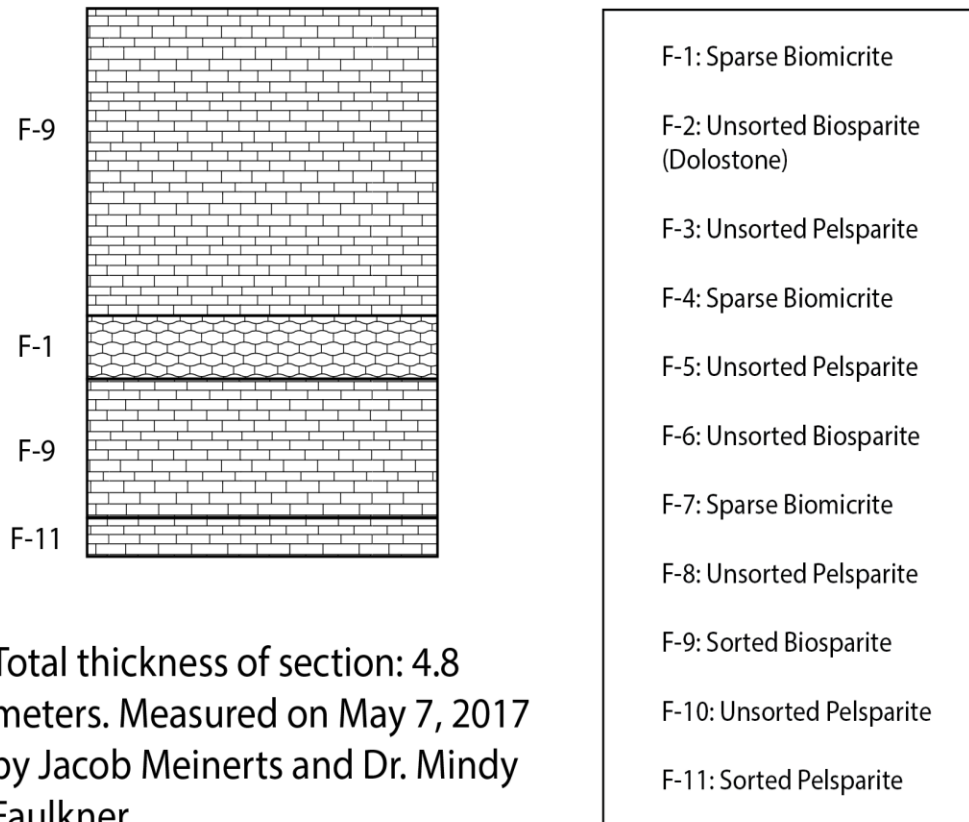


Figure 14: Column of measured section 14 with microfacies labels.

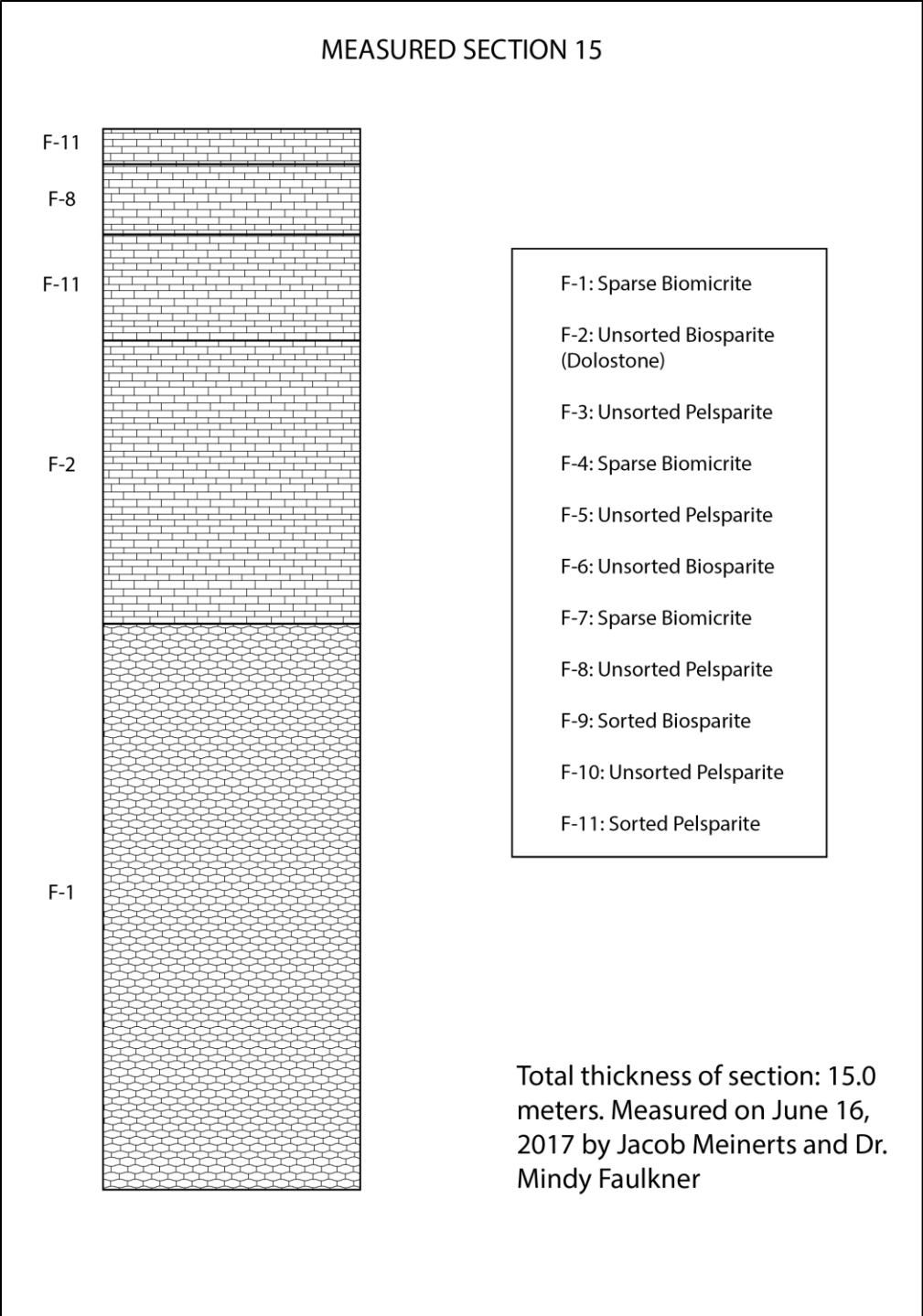
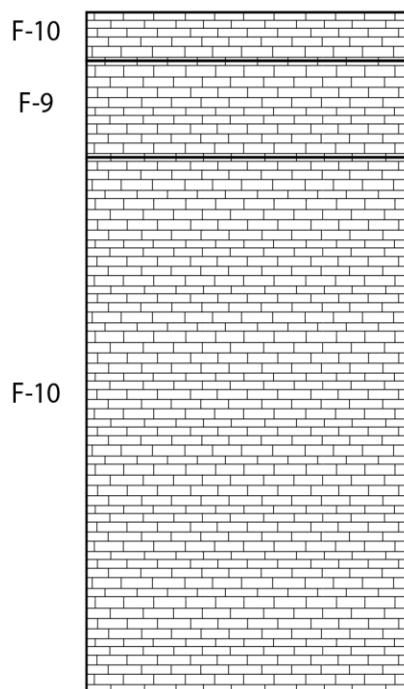


Figure 15: Column of measured section 15 with microfacies labels.

## MEASURED SECTION 16



Total thickness of section: 9.08 meters. Measured on November 3, 2017 by Jacob Meinerts and Dr. Mindy Faulkner

- F-1: Sparse Biomicrite
- F-2: Unsorted Biosparite (Dolostone)
- F-3: Unsorted Pelsparite
- F-4: Sparse Biomicrite
- F-5: Unsorted Pelsparite
- F-6: Unsorted Biosparite
- F-7: Sparse Biomicrite
- F-8: Unsorted Pelsparite
- F-9: Sorted Biosparite
- F-10: Unsorted Pelsparite
- F-11: Sorted Pelsparite

Figure 16: Column of measured section 16 with microfacies labels.

## **APPENDIX C: THIN SECTION ANALYSES**

### **Introduction**

Fifteen billets were shipped to Spectrum Petrographics for thin section preparation. The samples were stained with Alizarin red for calcite identification, and cut to three microns using quartz as the standard. After thoroughly looking over the thin sections to become familiar with the allochems, matrix, and other features within them, point counts were conducted to determine the composition of the thin sections and the Folk classification for each microfacies. Three hundred (300) points were used for each point count, the counts were done as traverses across the thin section horizontally, using a mechanical stage to keep all movements precise and unbiased.

The thin sections were looked at using a LABOMED Lx 400P research microscope, they were viewed in plane polarized light as well as cross polarized light, and a gypsum plate was also used to look at birefringence. The following tables show microphotographs of each thin section, one in plane polarized light (PPL) and one in cross polarized light (XPL), each microphotograph is viewed in 4x magnification. The tables show Folk classification, data about allochems, matrix, cements, bioturbation, diagenetic history, formation, and microfacies classification.

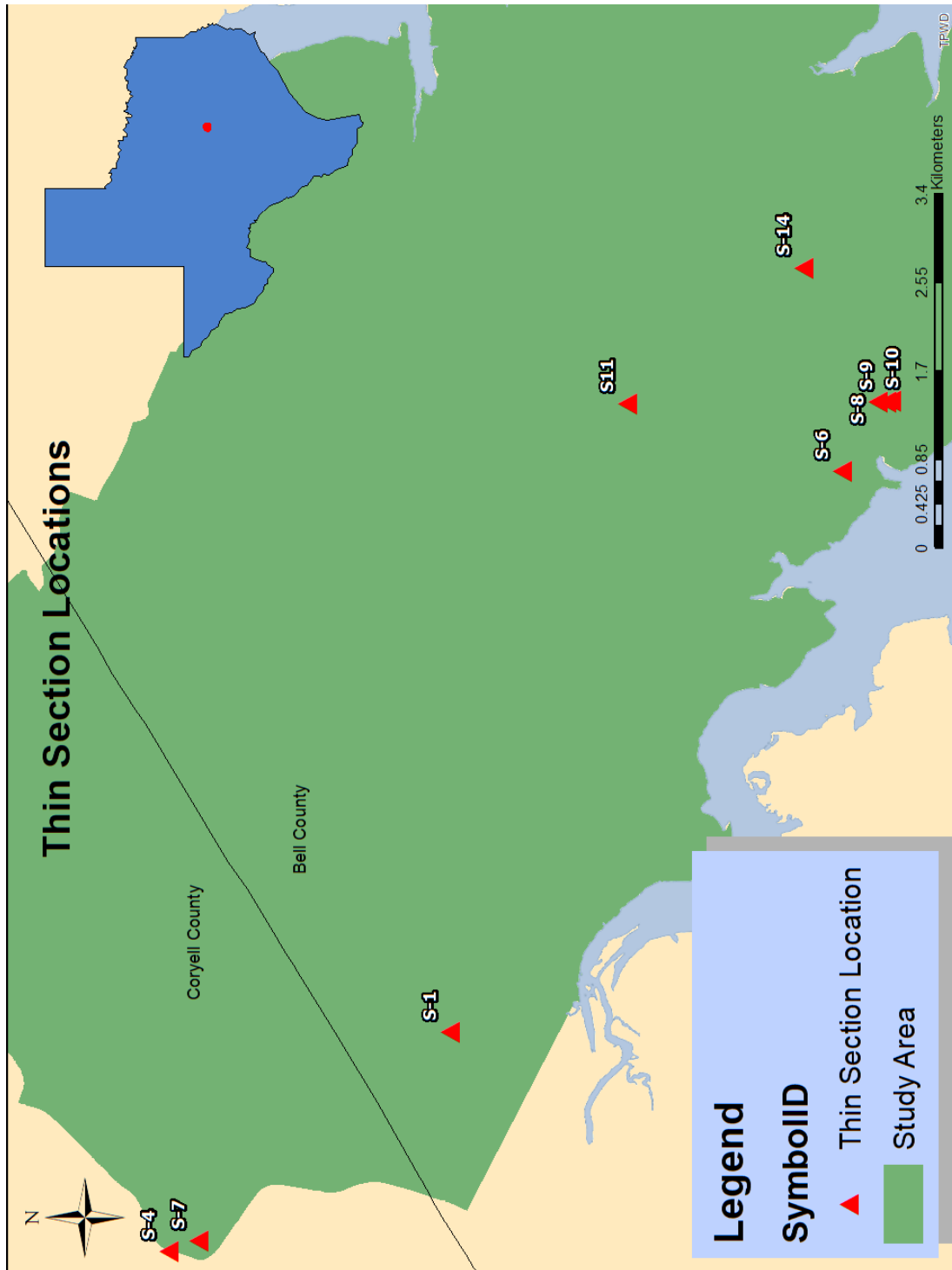


Figure C-1: Map of Owl Mountain Province showing locations of each thin section. Source: ArcGIS online database.

Table C-1: Microphotographs and classification for thin section JM1.

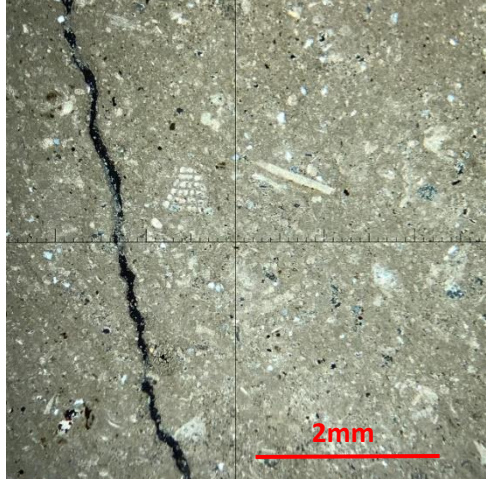
 <p style="text-align: center;">PPL</p>	 <p style="text-align: center;">XPL</p>
<p>Sample: JM01; 4x magnification</p>	
<p>Folk Classification: Sparse Biomicrite</p>	
<p>Allochems: Bivalves (4%), Peloids (3%), Gastropods (2%), Echinoids (1%)</p>	
<p>Matrix/Cement:            -Matrix: micrite (84%)            -Cement: calcite (5%)</p>	
<p>Dolomitization: N/A</p>	
<p>Porosity: fracture (&lt;1%), moldic (&lt;1%)</p>	
<p>Bioturbation: 4</p>	
<p>Diagenesis: 1) Deposition of allochems and micrite, 2) precipitation of microspar calcite, 3) micritization, 4) neomorphism of high Mg calcite/aragonite to low Mg calcite, 5) neomorphism of micrite to equant spar calcite, 6) recrystallization of some microspar and equant cements, 7) burial; compaction 8) dissolution of some allochems, 9) first phase dolomitization, 10) some de-dolomitization, 11) infill of pores with massive equant spar calcite, 12) fracture porosity, 13) oxidation of some allochems and grains.</p>	
<p>Formation: Edwards</p>	
<p>Facies: Shallow Peritidal – Sparse Bioclastic Mud Flat Microfacies (F-1)</p>	

Table C-2: Microphotographs and classification for thin section JM2.

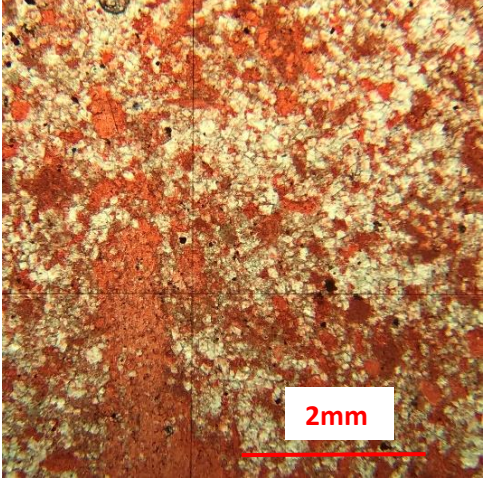
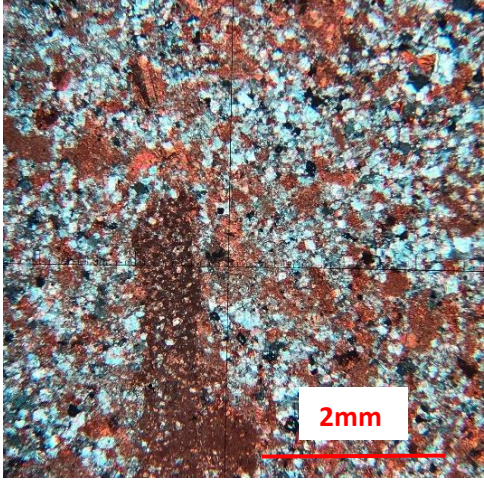
 <p style="text-align: center;">PPL</p>	 <p style="text-align: center;">XPL</p>
<p>Sample: JM02; 4x magnification</p>	
<p>Folk Classification: Unsorted Biosparite</p>	
<p>Allochems: Bivalves (1%), Peloids (1%), Echinoids (&lt;1%)</p>	
<p>Matrix/Cement:            -Matrix: micrite (28%)            -Cement: dolomite (71%), calcite (7%)</p>	
<p>Dolomitization: rhombic and microdolomite</p>	
<p>Porosity: Moldic (&lt;1%),</p>	
<p>Bioturbation: 3</p>	
<p>Diagenesis: 1) deposition of allochems and micrite, 2) precipitation of microspar calcite, 3) micritization, 4) neomorphism of high Mg calcite and aragonite to low Mg calcite, 5) neomorphism of some micrite to equant calcite cement, 6) recrystallization of some equant and microspar, 7) dolomitization, 8) burial; compaction, 9) limited pressure solution; suturing of grains, 10) infill of some pore space with equant spar calcite, 11) oxidation of some allochems and grains.</p>	
<p>Formation: Edwards</p>	
<p>Facies: Shallow Peritidal – Dolomite Mud Flat Microfacies (F-2)</p>	

Table C-3: Microphotographs and classification for thin section JM3.

PPL	XPL
Sample: JM03; 4x magnification	
Folk Classification: Unsorted Peloid Biosparite	
Allochems: Peloids (75%), Bivalves (1%), Gastropods (<1%)	
Matrix/Cement: -Matrix: micrite (7%) -Cement: calcite (3%), dolomite (<1%)	
Dolomitization: rhombic	
Porosity: moldic (8%), solutional (4%)	
Bioturbation: 5-6	
Diagenesis: 1) deposition of allochems and micrite, 2) precipitation of microspar calcite, 3) micritization, 4) precipitation of isopachous cement around some allochems, 5) neomorphism of high Mg calcite and aragonite to low Mg calcite, 6) neomorphism of some microspar to equant spar calcite, 7) recrystallization of some isopachous and equant cement, 8) burial; compaction, 9) dissolution of some allochems; creates moldic to solutional (vuggy) porosity, 10) first phase of dolomitization, 11) limited pressure solution; suturing of grains, 12) de-dolomitization of some allochems; creates more porosity, 13) second dolomitization phase with limited silicification of some allochems from hydrothermal activities, 14) dissolution; creates solutional porosity; some meteoric cements (meniscus), 15) oxidation of some allochems and grains.	
Formation: Edwards	
Facies: Shallow Subtidal – Peloidal Shoal Microfacies (F-3)	

Table C-4: microphotographs and classification for thin section JM4.

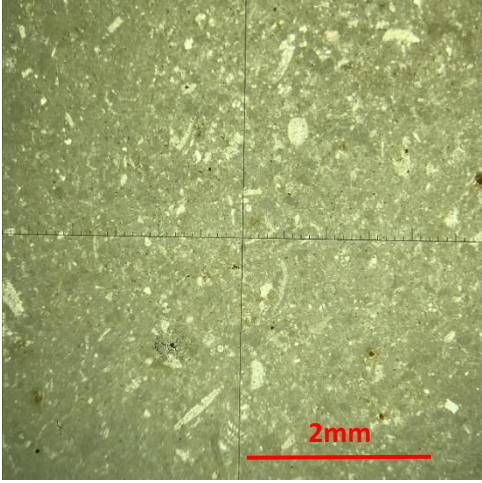
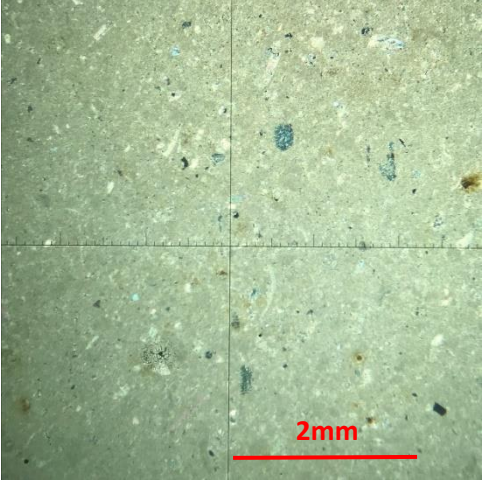
 <p style="text-align: center;">PPL</p>	 <p style="text-align: center;">XPL</p>
<p>Sample: JM-04; 4x magnification</p>	
<p>Folk Classification: Sparse Biomicrite</p>	
<p>Allochems: Bivalves (4%), Gastropods (3%), Peloids (2%), Echinoderms (1%)</p>	
<p>Matrix/Cement:            -Matrix: Micrite (89%)            -Cement: Calcite (&lt;1%), Dolomite (&lt;1%)</p>	
<p>Dolomitization: Rhombic</p>	
<p>Porosity: Fracture (&lt;1%)</p>	
<p>Bioturbation: 4</p>	
<p>Diagenesis: 1) deposition of allochems and micrite, 2) precipitation of microspar calcite, 3) micritization, 4) neomorphism of high Mg calcite and aragonite to low Mg calcite, 5) neomorphism of some microspar to equant spar calcite, 6) recrystallization of some isopachous and equant cement, 7) burial; compaction, 8) dissolution of some allochems; creates moldic to solutional (vuggy) porosity, 9) first phase of dolomitization, 10) limited pressure solution; suturing of grains, 11) de-dolomitization of some allochems; creates more porosity, 12) second dolomitization phase with limited silicification of some allochems from hydrothermal activities, 13) de-dolomitization of some allochems, 14) oxidation of some allochems and grains.</p>	
<p>Formation: Edwards</p>	
<p>Facies: Shallow Peritidal – Sparse Bioclastic Mud Flat Microfacies (F-1)</p>	

Table C-5: microphotographs and classification for thin section JM5.

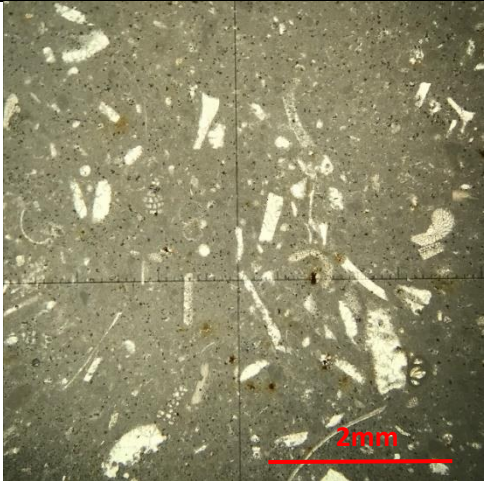
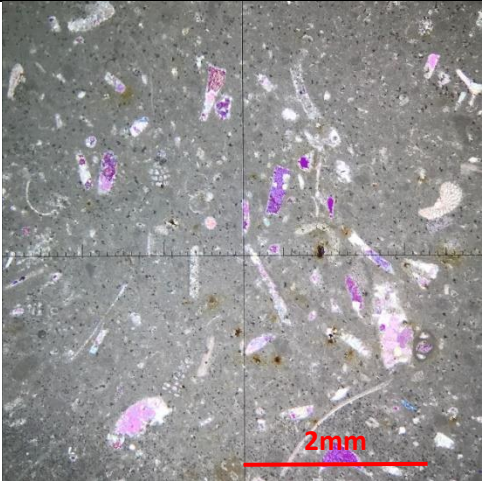
 <p style="text-align: center;">PPL</p>	 <p style="text-align: center;">XPL</p>
<p>Sample: JM-05; 4x magnification</p>	
<p>Folk Classification: Sparse Biomicrite</p>	
<p>Allochems: Bivalves (8%), Gastropods (2%), Echinoderms (1%), Bryozoa (&lt;1%), Foraminifera (&lt;1%)</p>	
<p>Matrix/Cement:          -Matrix: Micrite (87%)          -Cement: Calcite (&lt;1%)</p>	
<p>Dolomitization: N/A</p>	
<p>Porosity: Fracture (&lt;1%), Moldic (&lt;1%)</p>	
<p>Bioturbation: 3</p>	
<p>Diagenesis: 1) deposition of allochems and micrite, 2) precipitation of microspar calcite, 3) micritization, 4) neomorphism of high Mg calcite and aragonite to low Mg calcite, 5) neomorphism of some microspar to equant spar calcite, 6) recrystallization of some microspar and equant cement, 7) burial; compaction, 8) dissolution of some allochems; creates moldic to solutional (vuggy) porosity, 9) limited pressure solution; suturing of grains, 10) infill of pore space with massive equant spar calcite 11) limited dolomitization and silicification of some allochems; baroque dolomite; hydrothermal 12) de-dolomitization, 13) dissolution; creates solutional porosity 14) oxidation of some allochems and grains.</p>	
<p>Formation: Edwards</p>	
<p>Facies: Shallow Peritidal - Bivalve Mud Flat Microfacies (F-4)</p>	

Table C-6: microphotographs and classification for thin section JM6.

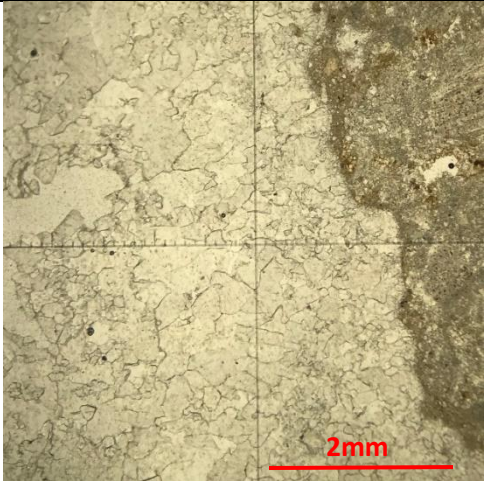
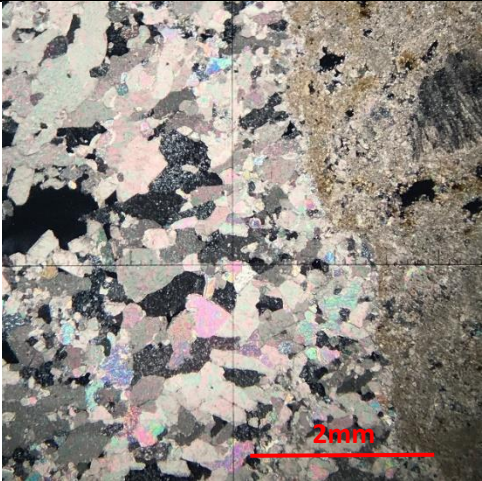
 <p style="text-align: center;">PPL</p>	 <p style="text-align: center;">XPL</p>
<p>Sample: JM-06; 4x magnification</p>	
<p>Folk Classification: Unsorted Pelsparite</p>	
<p>Allochems: Peloids (4%)</p>	
<p>Matrix/Cement:          -Matrix: Micrite (19%)          -Cement: Calcite (64%) Dolomite (&lt;1%)</p>	
<p>Dolomitization: Rhombic and microdolomite</p>	
<p>Porosity: Vuggy (9%), Moldic (5%)</p>	
<p>Bioturbation: 5-6</p>	
<p>Diagenesis: 1) deposition of allochems and micrite, 2) precipitation of microspar calcite, 3) micritization, 4) precipitation of isopachous cement around some allochems, 5) neomorphism of high Mg calcite and aragonite to low Mg calcite, 6) neomorphism of some microspar to equant spar calcite, 7) recrystallization of some isopachous and equant cement, 8) burial; compaction, 9) dissolution of some allochems; creates moldic to solutional (vuggy) porosity, 10) first phase of dolomitization, 11) limited pressure solution; suturing of grains, 12) de-dolomitization of some allochems; creates more porosity, 13) infill or pore spaces with massive equant spar calcite, 14) second dolomitization phase with limited silicification of some allochems from hydrothermal activities, 15) de-dolomitization, 16) fracture porosity, 17) dissolution; creates solutional porosity; some meteoric cements (meniscus), 18) oxidation of some allochems and grains.</p>	
<p>Formation: Edwards</p>	
<p>Facies: Shallow Subtidal – Marginal Mud Flat/Lagoon Microfacies (F-5)</p>	

Table C7: microphotographs and classification for thin section JM7.

 <p style="text-align: center;">PPL</p>	 <p style="text-align: center;">XPL</p>
<p>Sample: JM-07; 4x magnification</p>	
<p>Folk Classification: Unsorted Biosparite</p>	
<p>Allochems: Bivalves (17%), Peloids (12%), Echinoderms (2%), Foraminifera (&lt;1%), Algae (&lt;1%), Bryozoans (&lt;1%)</p>	
<p>Matrix/Cement:          -Matrix: Micrite (49%)          -Cement: Calcite (5%), Dolomite (2%)</p>	
<p>Dolomitization: Rhombic and Microdolomite</p>	
<p>Porosity: Vuggy (7%), Moldic (5%)</p>	
<p>Bioturbation: 4-5</p>	
<p>Diagenesis: 1) deposition of allochems and micrite, 2) precipitation of microspar calcite, 3) micritization, 4) precipitation of isopachous cement around some allochems, 5) neomorphism of high Mg calcite and aragonite to low Mg calcite, 6) neomorphism of some microspar to equant spar calcite, 7) recrystallization of some isopachous and equant cement, 8) burial; compaction, 9) dissolution of some allochems; creates moldic to solutional (vuggy) porosity, 10) first phase of dolomitization, 11) limited pressure solution; suturing of grains, 12) de-dolomitization of some allochems; creates more porosity, (13) fracture porosity, 14) dissolution; creates solutional porosity; some meteoric cements (meniscus), 15) oxidation of some allochems and grains.</p>	
<p>Formation: Edwards</p>	
<p>Facies: Shallow Subtidal – Bivalve Biohermal Microfacies (F-6)</p>	

Table C-8: microphotographs and classification for thin section JM8.

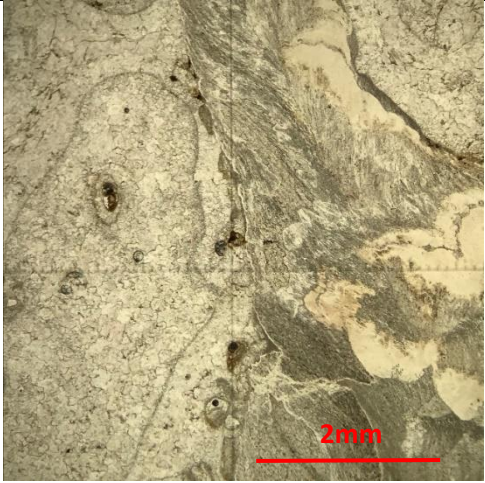
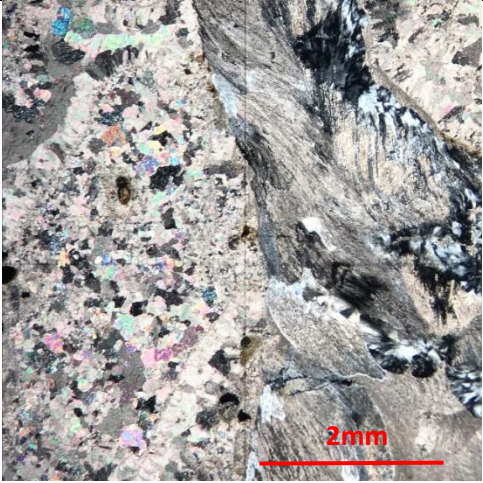
 <p style="text-align: center;">PPL</p>	 <p style="text-align: center;">XPL</p>
<p>Sample: JM-08; 4x magnification</p>	
<p>Folk Classification: Unsorted Biosparite</p>	
<p>Allochems: Bivalves (4%), Peloids (2%), Foraminifera (&lt;1%),</p>	
<p>Matrix/Cement:          -Matrix: Micrite (5%)          -Cement: Calcite (84%), Dolomite (1%), Iron oxide (1%), Opal Quartz (&lt;1%)</p>	
<p>Dolomitization: Rhombic and Microdolomite</p>	
<p>Porosity: Moldic (2%), Vuggy (1%)</p>	
<p>Bioturbation: 5-6</p>	
<p>Diagenesis: 1) deposition of allochems and micrite, 2) precipitation of microspar calcite, 3) micritization, 4) precipitation of isopachous cement around some allochems, 5) neomorphism of high Mg calcite and aragonite to low Mg calcite, 6) neomorphism of some microspar to equant spar calcite, 7) recrystallization of some isopachous and equant cement, 8) burial; compaction, 9) dissolution of some allochems; creates moldic to solutional (vuggy) porosity, 10) first phase of dolomitization, 11) limited pressure solution; suturing of grains, 12) de-dolomitization of some allochems; creates more porosity, 13) infill or pore spaces with massive equant spar calcite, 14) second dolomitization phase with limited silicification of some allochems from hydrothermal activities, 15) de-dolomitization, 16) fracture porosity, 17) dissolution; creates solutional porosity; some meteoric cements (meniscus), 18) oxidation of some allochems and grains.</p>	
<p>Formation: Edwards</p>	
<p>Facies: Shallow Subtidal – Bioherm Flank Microfacies (F-8)</p>	

Table C-9: microphotographs and classification for thin section JM9.

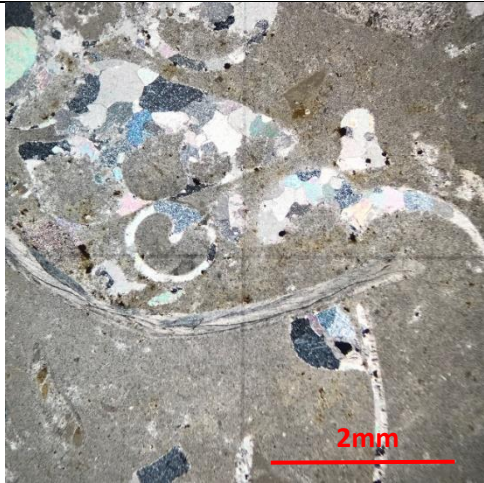
 <p style="text-align: center;">PPL</p>	 <p style="text-align: center;">XPL</p>
<p>Sample: JM-09; 4x magnification</p>	
<p>Folk Classification: Sparse Biomicrite</p>	
<p>Allochems: Gastropods (17%), Bivalves (16%), Algae (&lt;1%), Bryozoan (&lt;1%), Coral (&lt;1%)</p>	
<p>Matrix/Cement:          -Matrix: Micrite (60%)          -Cement: Iron oxide (6%)</p>	
<p>Dolomitization: N/A</p>	
<p>Porosity: Moldic (&lt;1%)</p>	
<p>Bioturbation: 3</p>	
<p>Diagenesis: 1) deposition of allochems and micrite, 2) precipitation of microspar calcite, 3) micritization, 4) neomorphism of high Mg calcite and aragonite to low Mg calcite, 5) neomorphism of some microspar to equant spar calcite, 6) recrystallization of some isopachous and equant cement, 7) burial; compaction, 8) dissolution of some allochems; creates moldic to solutional (vuggy) porosity, 9) limited pressure solution; suturing of grains, 10) infill or pore spaces with massive equant spar calcite, 11) second dolomitization phase with limited silicification of some allochems from hydrothermal activities, 12) de-dolomitization, 13) dissolution; creates solutional porosity; some meteoric cements (meniscus), 14) oxidation of some allochems and grains.</p>	
<p>Formation: Edwards</p>	
<p>Facies: Shallow Peritidal – Gastropod Mud Flat Microfacies (F-7)</p>	

Table C-10: microphotographs and classification for thin section JM10.

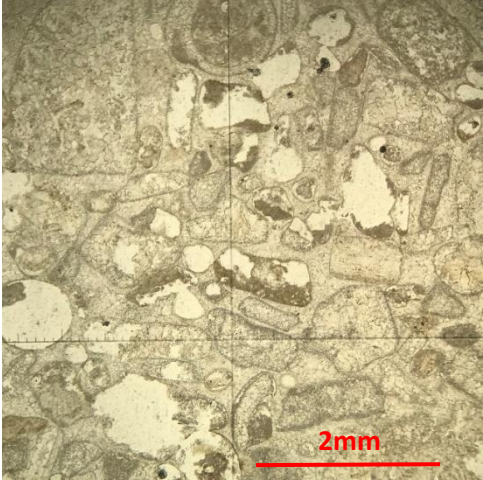
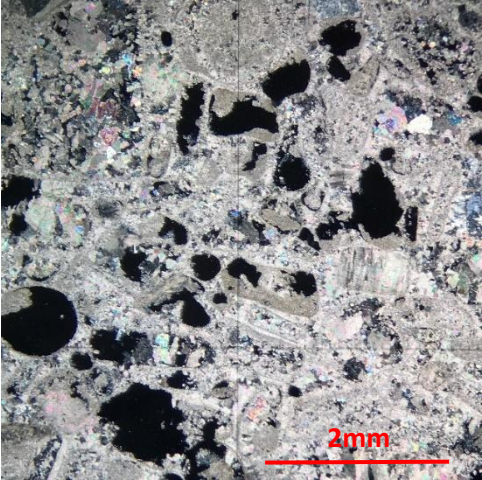
	
<p>PPL <span style="margin-left: 300px;">XPL</span></p>	
<p>Sample: JM-10; 4x magnification</p>	
<p>Folk Classification: Unsorted Biosparite</p>	
<p>Allochems: Bivalves (3%), Peloids (2%)</p>	
<p>Matrix/Cement:          -Matrix: Micrite (22%)          -Cement: Calcite (57%), Dolomite (1%)</p>	
<p>Dolomitization: Rhombic and Microdolomite</p>	
<p>Porosity: Moldic (11%), Vuggy (4%)</p>	
<p>Bioturbation: 4-5</p>	
<p>Diagenesis: 1) deposition of allochems and micrite, 2) precipitation of microspar calcite, 3) micritization, 4) neomorphism of high Mg calcite and aragonite to low Mg calcite, 5) neomorphism of some microspar to equant spar calcite, 6) recrystallization of some isopachous and equant cement, 7) burial; compaction, 8) dissolution of some allochems; creates moldic to solutional (vuggy) porosity, 9) first phase of dolomitization, 10) limited pressure solution; suturing of grains, 11) de-dolomitization of some allochems; creates more porosity, 12) infill or pore spaces with massive equant spar calcite, 13) second dolomitization phase with limited silicification of some allochems from hydrothermal activities, 14) de-dolomitization, 15) fracture porosity, 16) dissolution; creates solutional porosity; some meteoric cements (meniscus), 17) oxidation of some allochems and grains.</p>	
<p>Formation: Edwards</p>	
<p>Facies: Shallow Subtidal –Bioherm Flank Microfacies (F-8)</p>	

Table C-11: microphotographs and classification for thin section JM11.

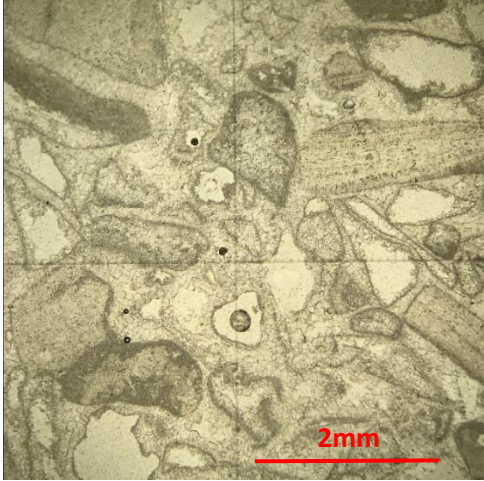
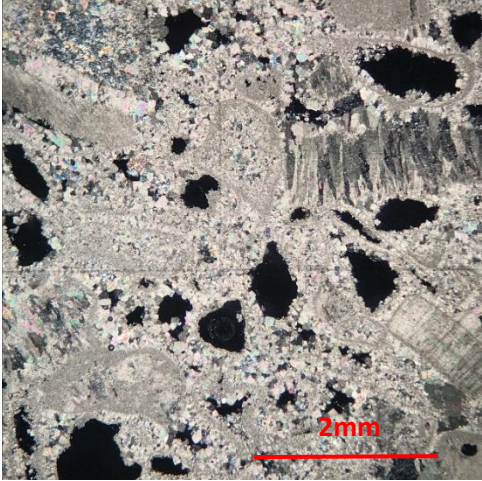
	
<p>PPL <span style="margin-left: 300px;">XPL</span></p>	
<p>Sample: JM-11; 4x magnification</p>	
<p>Folk Classification: Unsorted Biosparite</p>	
<p>Allochems: Bivalves (7%), Peloids (1%), Bryozoan (&lt;1%)</p>	
<p>Matrix/Cement:          -Matrix: Micrite (9%)          -Cement: Calcite (65%), Dolomite (&lt;1%)</p>	
<p>Dolomitization: Rhombic and Microdolomite</p>	
<p>Porosity: Vuggy (16%), Moldic (6%)</p>	
<p>Bioturbation: 4-5</p>	
<p>Diagenesis: 1) deposition of allochems and micrite, 2) precipitation of microspar calcite, 3) micritization, 4) precipitation of isopachous cement around some allochems, 5) neomorphism of high Mg calcite and aragonite to low Mg calcite, 6) neomorphism of some microspar to equant spar calcite, 7) recrystallization of some isopachous and equant cement, 8) burial; compaction, 9) dissolution of some allochems; creates moldic to solutional (vuggy) porosity, 10) first phase of dolomitization, 11) de-dolomitization of some allochems; creates more porosity, 12) infill or pore spaces with massive equant spar calcite, 13) second dolomitization phase with limited silicification of some allochems from hydrothermal activities, 14) de-dolomitization, 15) dissolution; creates solutional porosity; some meteoric cements (meniscus), 16) oxidation of some allochems and grains.</p>	
<p>Formation: Edwards</p>	
<p>Facies: Shallow Subtidal –Bioherm Flank Microfacies (F-8)</p>	

Table C-12: microphotographs and classification for thin section JM12.

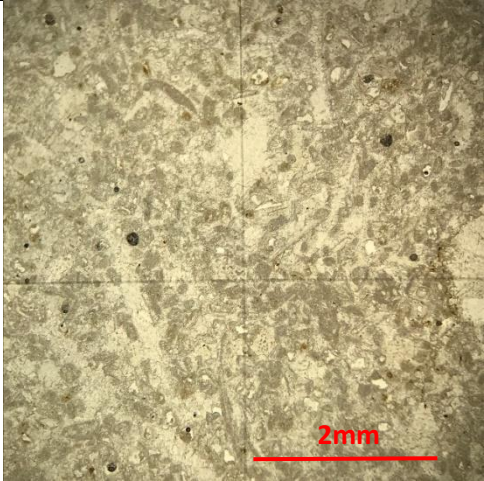
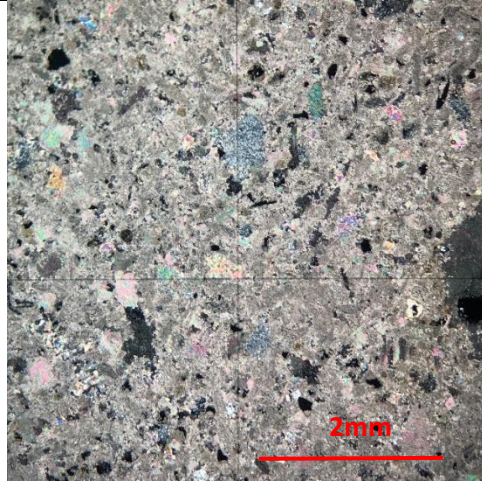
 <p style="text-align: center;">PPL</p>	 <p style="text-align: center;">XPL</p>
<p>Sample: JM-12; 4x magnification</p>	
<p>Folk Classification: Unsorted Pelsparite</p>	
<p>Allochems: Peloids (35%), Bryozoan (1%), Bivalves (1%), Gastropods (1%), Algae (&lt;1%)</p>	
<p>Matrix/Cement:          -Matrix: Micrite (2%)          -Cement: Calcite (46%), Dolomite (8%), Gypsum (&lt;1%), Iron oxide (&lt;1%)</p>	
<p>Dolomitization: Rhombic and Microdolomite</p>	
<p>Porosity: Moldic (4%), Vuggy (1%)</p>	
<p>Bioturbation: 5</p>	
<p>Diagenesis: 1) deposition of allochems and micrite, 2) precipitation of microspar calcite, 3) micritization, 4) precipitation of isopachous cement around some allochems, 5) neomorphism of high Mg calcite and aragonite to low Mg calcite, 6) neomorphism of some microspar to equant spar calcite, 7) recrystallization of some isopachous and equant cement, 8) burial; compaction, 9) dissolution of some allochems; creates moldic to solutional (vuggy) porosity, 10) first phase of dolomitization, 11) limited pressure solution; suturing of grains, 12) de-dolomitization of some allochems; creates more porosity, 13) infill or pore spaces with massive equant spar calcite, 14) second dolomitization phase with limited silicification of some allochems from hydrothermal activities, 15) de-dolomitization, 16) fracture porosity, 17) dissolution; creates solutional porosity; some meteoric cements (meniscus), 18) oxidation of some allochems and grains.</p>	
<p>Formation: Edwards</p>	
<p>Facies: Shallow Subtidal – Sheltered Backreef/Bioherm Peloidal Microfacies (F-10)</p>	

Table C-13: microphotographs and classification for thin section JM13.

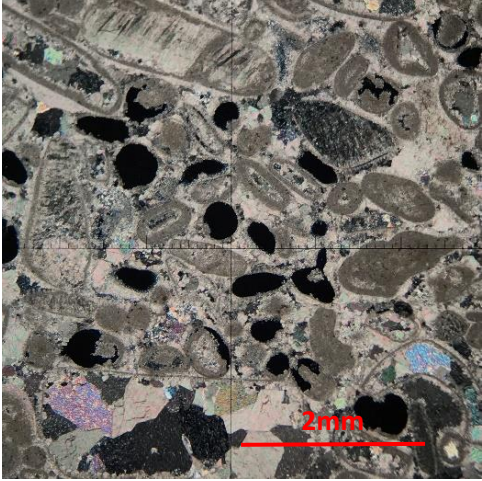
 <p style="text-align: center;">PPL</p>	 <p style="text-align: center;">XPL</p>
<p>Sample: JM-13; 4x magnification</p>	
<p>Folk Classification: Sorted Pelsparite</p>	
<p>Allochems: Peloids (19%), Ooids (13%), Bivalves (4%), Algae (1%), Bryozoan (&lt;1%)</p>	
<p>Matrix/Cement:          -Matrix: Micrite (5%)          -Cement: Calcite (47%), Dolomite (1%), Iron oxide (&lt;1%)</p>	
<p>Dolomitization: Rhombic and Microdolomite</p>	
<p>Porosity: Moldic (7%), Vuggy (2%)</p>	
<p>Bioturbation: 5</p>	
<p>Diagenesis: 1) deposition of allochems and micrite, 2) precipitation of microspar calcite, 3) micritization, 4) precipitation of isopachous cement around some allochems, 5) neomorphism of high Mg calcite and aragonite to low Mg calcite, 6) neomorphism of some microspar to equant spar calcite, 7) recrystallization of some isopachous and equant cement, 8) burial; compaction, 9) dissolution of some allochems; creates moldic to solutional (vuggy) porosity, 10) first phase of dolomitization, 11) de-dolomitization of some allochems; creates more porosity, 12) infill or pore spaces with massive equant spar calcite, 13) second dolomitization phase with limited silicification of some allochems from hydrothermal activities, 14) de-dolomitization, 15) dissolution; creates solutional porosity; some meteoric cements (meniscus), 16) oxidation of some allochems and grains.</p>	
<p>Formation: Edwards</p>	
<p>Facies: Shallow Subtidal – Channel Peloidal Microfacies (F-11)</p>	

Table C-14: microphotographs and classification for thin section JM14.

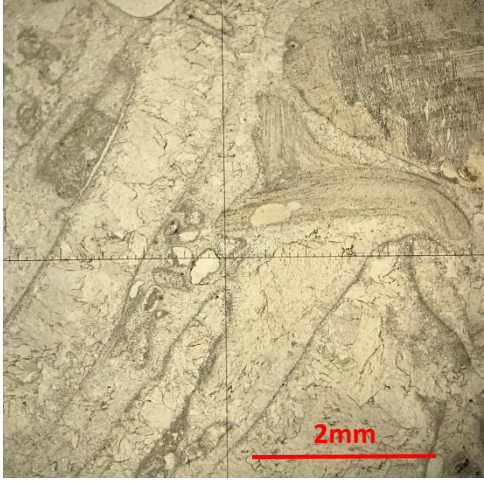
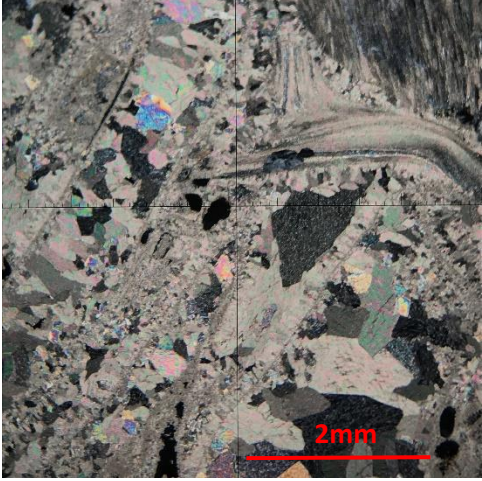
 <p style="text-align: center;">PPL</p>	 <p style="text-align: center;">XPL</p>
<p>Sample: JM-14; 4x magnification</p>	
<p>Folk Classification: Sorted Biosparite</p>	
<p>Allochems: Bivalves (6%), Peloids (4%)</p>	
<p>Matrix/Cement:          -Matrix: Micrite (9%)          -Cement: Calcite (60%), Dolomite (10%), Opal Quartz (3%), Iron oxide (&lt;1%)</p>	
<p>Dolomitization: Rhombic and Microdolomite</p>	
<p>Porosity: Vuggy (6%), Moldic (2%)</p>	
<p>Bioturbation: 4-5</p>	
<p>Diagenesis: 1) deposition of allochems and micrite, 2) precipitation of microspar calcite, 3) micritization, 4) precipitation of isopachous cement around some allochems, 5) neomorphism of high Mg calcite and aragonite to low Mg calcite, 6) neomorphism of some microspar to equant spar calcite, 7) recrystallization of some isopachous and equant cement, 8) burial; compaction, 9) dissolution of some allochems; creates moldic to solutional (vuggy) porosity, 10) first phase of dolomitization, 11) limited pressure solution; suturing of grains, 12) de-dolomitization of some allochems; creates more porosity, 13) infill or pore spaces with massive equant spar calcite, 14) second dolomitization phase with limited silicification of some allochems from hydrothermal activities, 15) de-dolomitization, 16) fracture porosity, 17) dissolution; creates solutional porosity; some meteoric cements (meniscus), 18) oxidation of some allochems and grains.</p>	
<p>Formation: Edwards</p>	
<p>Facies: Shallow Subtidal – Inter-Bioherm Channel Microfacies (F-9)</p>	

Table C-15: microphotographs and classification for thin section JM15.

<p>PPL <span style="margin-left: 300px;">XPL</span></p>	
Sample: JM-15; 4x magnification	
Folk Classification: Sorted Biosparite	
Allochems: Bivalves (6%), Peloids (4%), Algae (<1%)	
Matrix/Cement:	
<ul style="list-style-type: none"> <li>-Matrix: Micrite (4%)</li> <li>-Cement: Calcite (44%), Opal Quartz (35%), Dolomite (6%)</li> </ul>	
Dolomitization: Rhombic and Microdolomite	
Porosity: Moldic (<1%), Vuggy (<1%)	
Bioturbation: 4-5	
<p>Diagenesis: 1) deposition of allochems and micrite, 2) precipitation of microspar calcite, 3) micritization, 4) precipitation of isopachous cement around some allochems, 5) neomorphism of high Mg calcite and aragonite to low Mg calcite, 6) neomorphism of some microspar to equant spar calcite, 7) recrystallization of some isopachous and equant cement, 8) burial; compaction, 9) dissolution of some allochems; creates moldic to solutional (vuggy) porosity, 10) first phase of dolomitization, 11) limited pressure solution; suturing of grains, 12) de-dolomitization of some allochems; creates more porosity, 13) infill or pore spaces with massive equant spar calcite, 14) second dolomitization phase with limited silicification of some allochems from hydrothermal activities, 15) de-dolomitization, 16) fracture porosity, 17) dissolution; creates solutional porosity; some meteoric cements (meniscus), 18) oxidation of some allochems and grains.</p>	
Formation: Edwards	
Facies: Shallow Subtidal – Inter-Bioherm Channel Microfacies (F-9)	

## VITA

Jacob A. Meinerts graduated from Springtown High School in Springtown, Texas in 2011. Jacob graduated from Stephen F. Austin State University where he received his Bachelor of Science in Geology. In August of 2016 he was admitted into the Graduate School of Stephen F. Austin State University to pursue a Master of Science degree in Geology. Jacob received his Master of Science Degree in December of 2018.

Permanent Address:       308 Goshen Road  
                                      Springtown, Texas, 76082

Style used: Geological Society of America

This thesis was typed by Jacob A. Meinerts